INFORMATION TO USERS

This manuscript has been reproduced from the microfilm master. UMI films the text directly from the original or copy submitted. Thus, some thesis and dissertation copies are in typewriter face, while others may be from any type of computer printer.

The quality of this reproduction is dependent upon the quality of the copy submitted. Broken or indistinct print, colored or poor quality illustrations and photographs, print bleedthrough, substandard margins, and improper alignment can adversely affect reproduction.

In the unlikely event that the author did not send UMI a complete manuscript and there are missing pages, these will be noted. Also, if unauthorized copyright material had to be removed, a note will indicate the deletion.

Oversize materials (e.g., maps, drawings, charts) are reproduced by sectioning the original, beginning at the upper left-hand corner and continuing from left to right in equal sections with small overlaps. Each original is also photographed in one exposure and is included in reduced form at the back of the book.

Photographs included in the original manuscript have been reproduced xerographically in this copy. Higher quality 6" x 9" black and white photographic prints are available for any photographs or illustrations appearing in this copy for an additional charge. Contact UMI directly to order.

UMI®

Bell & Howell Information and Learning
300 North Zeeb Road, Ann Arbor, MI 48106-1346 USA
800-521-0600

Defining the cis-acting requirements in the HMG-CoA reductase gene for karmellae biogenesis

by

Deborah Ann Profant

A dissertation submitted in partial fulfillment of the requirements for the degree of

Doctor of Philosophy

University of Washington

1999

Program Authorized to Offer Degree: Department of Zoology

Doctoral Dissertation

In presenting this thesis in partial fulfillment of the requirements for the Doctoral degree at the University of Washington, I agree that the Library shall make its copies freely available for inspection. I further agree that extensive copying of the dissertation is allowable only for scholarly purposes, consistent with "fair use" as prescribed in the U.S. Copyright Law. Requests for copying or reproduction of this dissertation may be referred to UMI Dissertation Services, 300 North Zeeb Road, P.O. Box 1346, Ann Arbor, MI 48106-1346, to whom the author has granted "the right to reproduce and sell (a) copies of the manuscript in microform and/or (b) printed copies of the manuscript made from microform."

Signature Deborah ann Profant

Date 5/11/99

University of Washington
Graduate School

This is to certify that I have examined this copy of a doctoral dissertation by

Deborah Ann Profant

and have found that it is complete and satisfactory in all respects,
and that any and all revisions required by the final
examining committee have been made.

Chair of Supervisory Committee:

Robin Wright
Robin Wright

Reading Committee:

Beth Traxler

Aimée Bakken
Aimée Bakken

Robin Wright
Robin Wright

Date: 5/11/99

University of Washington

Abstract

Defining the cis-acting requirements in the HMG-CoA reductase gene for karmellae biogenesis

by Deborah Ann Profant

Chairperson of the Supervisory Committee: Associate Professor Robin Wright
Department of Zoology

In yeast and mammalian cells, increased levels of the ER membrane protein, HMG-CoA reductase (HMGR), induce specific ER membrane arrays. Yeast express two HMGR isozymes, Hmg1p and Hmg2p, each of which induces a morphologically distinct proliferation of the ER. Hmg2p induces short stacks of ER membranes that may be found associated with the nucleus or be present at the cell periphery. Hmg1p induces karmellae, which are stacks of nuclear-associated membranes. The HMGR protein consists of two domains, a polytopic membrane domain at the amino terminus and a cytosolic catalytic domain at the carboxyl terminus. Experiments from our laboratory had indicated that the HMGR membrane domain was exclusively responsible for generation of ER membrane proliferations. We recently discovered that this conclusion is incorrect: sequences at the carboxyl terminus can in fact profoundly affect karmellae biogenesis. Specifically, truncations of Hmg1p that removed or shortened the carboxyl terminus were unable to induce karmellae. Our working hypothesis is that a truncated or misfolded cytosolic domain prevents proper signaling for karmellae biogenesis by interfering with the required tertiary structure of the membrane domain.

Additionally, our laboratory had previously determined that the last ER lumenal loop (Loop G) of the Hmg1p membrane domain contains a signal needed for proper assembly of karmellae. The folding of Loop G is likely to impact the lumenal interactions of the membrane domain, providing a signal when the conformation of this region permits one. Our goal is to determine the precise amino acid sequence needed for proper function of this signal. To this end, we have randomly mutagenized the Loop G sequence via mutagenic PCR, expressed the mutagenized Hmg1p in yeast, and screened for inability to properly generate karmellae. Analysis of Loop G sequences in karmellae-

defective as well as karmellae-competent mutants indicates that changes in charged residues of the Loop G region profoundly affect karmellae biogenesis. Our working hypothesis is that Loop G serves as a karmellae-inducing signal by mediating protein-protein interactions and that these charged amino acids may be important for maintaining the proper secondary structure of the Loop G region needed for these interactions.

TABLE OF CONTENTS

List of Figures

List of Tables

List of Abbreviations

ER: endoplasmic reticulum

HMGR: HMG-CoA reductase

$DiOC_6$: 3,3'-dihexyloxacarbocyanine iodide

CHX: cycloheximide

β-gal: β-galactosidase

mem: membrane domain

cat:: catalytic domain

Acknowledgments

The author wishes to thank her committee members Robin Wright, Aimee Bakken, Beth Traxler, and Trisha Davis for their support and suggestions. I thank my reading committee, Robin Wright, Aimee Bakken, and Beth Traxler for their comments and willingness to improve the content and style of the thesis. I thank Robin for being a patient advisor during my stay in her lab and for introducing me to the world of electron microscopy. I especially want to thank Barbara Wakimoto for her advice and willingness to listen when I was struggling to finish my degree.

My time in the Wright lab was greatly enhanced by my lab cohort. I thank Mark Parrish for his patience and his allocation of many hours for editing my drafts and figures. I am indebted to Ann Koning, Pek Lum, Chris Roberts, Steve Castillo, and Cosette LeCiel for providing guidance and friendship to me. I also want to thank the scientists who sent me strains and plasmids for my work: Randy Hampton, Stan Fields, Steve Elledge, Philip James, and Helen Cheng from the Simoni lab.

I want to thank my family and friends who supported me throughout my stay in Seattle and encouraged me to continue with school.

Dedication

The author wishes to dedicate this thesis to Judi, Mariya, and Mom who gave much love and understanding.

Chapter 1: Introduction

Membrane Function

A cell's survival depends on the structural integrity and function of its membranes. The plasma membrane allows selective exchange of materials with the environment while maintaining a boundary around the cellular contents. In eukaryotes, the evolution of internal membrane-bound organelles permitted compartmentalization necessary for specialized functions including secretion, breakdown of components, and the separation of transcription from translation. Two benefits of compartmentalization are additional regulation of interactions provided by the sequestration into a local environment and the separation of incompatible processes into separate organelles. The costs associated with compartmentalization are the requirement to effectively maintain inter-organelle communication and the requirement to sustain the identity of each organelle. Each organelle is usually characterized by a unique complement of structural proteins and enzymes and, to some extent, by a particular lipid composition.

How is the identity of each organelle maintained while extensive traffic occurs between organelles? A central problem for membrane biogenesis is the mechanism by which characteristic protein components of each membrane are maintained in the face of rapid turnover of the membranes. Another important consideration is how the asymmetric distribution of various proteins and lipid species is established and maintained in the different membranes. The membrane of each organelle is subdivided into domains whose composition and function can differ from the

neighboring region of the membrane. In other words, how do these subdomains within membranes remain intact? Membranes and organelles grow by expansion of existing structures. This fact implies that machinery exists which recognizes the organelle-targeting information on proteins and machinery exists which monitors changes in lipid composition in regions of the various membranes. Many questions remain in the area of lipid targeting and transport. Recent studies have shown that lipids can be rearranged within membranes by vesicle-mediated transport or by phospholipid transfer proteins (Wirtz and Zilversmit, 1968; Wirtz and Gadella, 1990).

Membrane Biogenesis

The ability of a cell to respond to signals from the environment or neighboring cells requires temporal and spatial regulation of membrane components. However, very little is known about the mechanisms that coordinate membrane biosynthesis and turnover. The study of cells programmed for specialized membrane biosynthesis may reveal the molecular mechanisms that underlie the regulation of membrane composition as documented in the examples that follow.

Specialized glial cells send out plasma membrane processes that become tightly wound around axons to form the myelin sheath. Myelin insulates nerve fibers to increase the velocity of the signal transmitted down the axon. The structure of myelin has been extensively studied and was determined to be a lipid bilayer sandwiched between two layers of protein. Numerous studies on myelin revealed that the protein components of myelin determine the extracellular spacing between the membranes and that the presence of many acidic lipid species is required to form the multilamellar structure (Morell, 1984). Lipid composition in myelin varies with age of the animal and between different regions of the nervous system. Cells adjust the cholesterol levels in

myelin in response to alterations in lipid composition (Morell, 1984). These studies on myelin indicate that membrane assembly is not only dictated by the protein components, but also by the lipid species.

In addition to plasma membrane alterations, cells can modulate their endoplasmic reticulum (ER) in response to environmental stimuli. Exposure to organic pollutants causes the proliferation of smooth ER in the digestive cells of marine bivalve molluscs. Besides ER changes, the molluscs alter the permeability of their lysosomal membranes in order to survive (Nott and Moore, 1987). In another study, European eels were examined for ultrastructural and biochemical alterations following a toxic spill in the Rhine river. The eels proliferated their smooth ER, mitochondria, peroxisomes, and lysosomes. The detoxifying enzymes present in these organelles were up-regulated, and the smooth ER proliferation was attributed to an increase in the level of cytochrome P450 protein (Braunbeck and Volkl, 1991).

Developmental programming can also lead to specialized membrane production. For example, B lymphocytes dramatically increase their rough ER in order to accomodate antibody production following exposure to antigen stimulation or mitogens (Shohat *et al.*, 1973; Zucker-Franklin *et al.*, 1988). Post-natal differentiation of rat hepatocytes leads to a rapid increase in smooth ER which will be needed for detoxification (Dallner *et al.*, 1966). Many cell types throughout the body can expand their ER in response to changing conditions. Some of these cell types, such as steroid-hormone producing cells of the adrenal cortex, have natural elevations in HMG-CoA reductase and assemble extra ER membrane arrays due to the increased level of the reductase protein (Sisson and Fahrenbach, 1967; Black, 1972).

Besides HMG-CoA reductase, a number of other ER-anchored proteins can induce proliferation of ER membranes when expressed at increased levels.

However, not all ER-anchored proteins are capable of eliciting the ER production response from the cell. The proteins, HMG-CoA reductase (Wright *et al.*, 1988), cytochrome P450 (Schunck *et al.*, 1991), cytochrome b5 (Vergeres *et al.*, 1993), canine ribosomal receptor (Wanker *et al.*, 1995), protease B negative 1 (Pbn1p) (Naik and Jones, 1998), and plant plasma membrane H^+-ATPase (Villalba *et al.*, 1992), can all induce ER proliferations in the yeast, *Saccharomyces cerevisiae,* but they do not share any sequence homologies. These proteins all have at least one ER-membrane spanning region but their total number of transmembrane-spanning regions varies from one to ten. What properties of these membrane proteins lead to the cell perceiving a signal for increased ER production? In this dissertation, I postulate that these different proteins use a common pathway to signal for ER proliferation. The ER proliferation pathway requires increased levels of an ER-anchored protein which assembles other lipids and proteins into an ER subcompartment, thereby modifying the composition of the ER. The cell perceives this altered ER composition as the signal for ER proliferation.

Prokaryotic cells are also capable of generating membrane proliferations in response to the overproduction of certain membrane proteins. High levels of fumurate reductase in *Escherichia coli* induced tubular membrane structures that branched internally from the cytoplasmic face of the cell's membrane (Weiner *et al.*, 1984). Fumurate reductase is composed of four nonidentical subunits; two of the subunits are membrane-bound proteins. The high level of fumurate reductase accounted for more than 50% of the inner membrane protein without reducing the levels of other membrane proteins. Weiner *et al.* determined that the amount of membrane lipid also increased such that the lipid/protein ratio remained constant. These authors postulated that membrane tubule formation required the ability to induce changes in phospholipid biosynthesis and they detected a large increase in cardiolipin, an increase in unsaturated

fatty acids, and a decrease in saturated fatty acids. A different lab noted a similar phenomenon with overproduction of *sn*-glycerol-3-phosphate acyltransferase, an integral membrane protein (Wilkison, 1986). This protein was overproduced 35 fold in *E. coli* and caused the formation of intracellular tubular structures that were closely associated with the cytoplasmic side of the plasma membrane. In contrast to the results with fumuarate reductase, *sn*-glycerol-3-phosphate acyltransferase elevation did not significantly change phospholipids. The most striking example of membrane induction occurred in response to a ten fold overproduction of the membrane-bound ATP synthase complex (Von Meyenburg *et al.*, 1984). The elevated levels of the ATP synthase complex resulted in an inhibition of cell division, and in formation of membrane vesicles and inclusion bodies. This result is the first documented case of membrane arrays leading to a cell growth phenotype; in most of the reported cases, cells accommodate the extra membranes well and do not display a growth phenotype (Wright *et al.*, 1988; Villalba *et al.*, 1992; Vergeres *et al.*, 1993; Wanker *et al*, 1995; Naik and Jones, 1998). Scientists have begun to explore the mechanisms that different cell types use to regulate the remodeling and expansion of their membranes and as discussed above, have focused on different models to study these alterations. In the following section, I will discuss the inducible membrane system known as karmellae which yeast cells assemble in response to elevations in HMG-CoA reductase.

Properties of HMG-CoA reductase

The best characterized example of the coordination between membrane protein synthesis and membrane assembly is the induction of membranes by the ER membrane protein, HMG-CoA (3-hydroxy-3-methylglutaryl Coenzyme A) reductase. In yeast and mammalian cells, elevations in the level of HMG-CoA reductase (HMGR)

lead to the assembly of cell-type specific ER membrane arrays. When a mammalian cell is treated with a competitive inhibitor of HMG-CoA reductase, the level of HMGR protein rises and induces the formation of crystalloid ER (Chin *et al.*, 1982). Crystalloid ER are hexagonal arrays of smooth membrane tubules, which house HMGR and at least 9 other proteins (Kochevar and Anderson, 1987). Twenty-five percent of the protein in crystalloid ER was HMG-CoA reductase, with one other protein detected at an equivalent level. The other seven proteins were less abundant (Kochevar and Anderson, 1987). In contrast to mammalian cells, yeast assemble nuclear-associated membrane stacks known as karmellae in response to increased levels of HMGR (Wright *et al.*, 1988). When human HMGR is expressed at increased levels in yeast, karmellae are still formed rather than crystalloid ER (Wright *et al.*, 1990). Thus the genetics of the cell, and not the specific protein, determine what type of membranes are formed. The ability to stimulate membrane synthesis by simply altering the amount of HMGR provides a sterling opportunity for scientists to analyze the regulation of ER structure and function as well as to learn more about the regulation of the HMGR protein.

In addition to triggering ER membrane biogenesis, HMG-CoA reductase catalyzes the rate-limiting step in sterol biosynthesis and is a target of drugs aimed at lowering cholesterol in humans (Goldstein and Brown, 1990). HMG-CoA reductase catalyzes the reduction of HMG-CoA to mevalonate. Mevalonate is the precursor for sterols as well as numerous non-sterol compounds (Figure 1.1). The sterols produced are important for maintaining membrane fluidity as well as leading to downstream molecules such as steroid hormones. The non-sterol isoprenoid compounds participate in many cellular processes such as electron transport (ubiquinones), photosynthesis (plastoquinones), signal transduction (farnesyl), and protein glycosylation (dolichols).

The structure of HMGR can be divided into two domains, the catalytic domain in the cytosol and the membrane domain. The yeast and mammalian HMGR isozymes are predicted to have a complex amino-terminal domain that passes through the ER bilayer eight times, followed by a non-conserved linker region and then the catalytic domain (Basson *et al.*, 1988; Roitelman *et al.*, 1992; Lum *et al.*, 1996). The membrane domain is responsible for the regulated degradation of both the mammalian and yeast HMGRs (Gil *et al.*, 1985; Jingami *et al.*, 1987; Hampton and Rine, 1994) and the proliferation of ER membranes when HMGR levels increase (Jingami *et al.*, 1987; Parrish *et al.*, 1995).

Unlike mammalian cells which have one HMGR, *Saccharomyces cerevisiae* expresses two functional HMGR isozymes, Hmg1p and Hmg2p (Basson *et al.*, 1986). Both isozymes produce mevalonate and can support cell survival alone without the other isozyme (Basson *et al.*, 1988). However, a study by Casey *et al.* suggested that the mevalonate produced from each isozyme is shunted into a separate, compartmentalized isoprenoid pathway. These authors found that palmitoleic acid acted as a positive regulator of only the Hmg1p isozyme. In contrast, Hmg2p was inhibited by oleic acid and was not regulated by palmitoleic acid (Casey *et al.*, 1992). The two *S. cerevisiae* isozymes share 46% identity in their membrane domains and 95% identity in their catalytic domains (Basson *et al.*, 1988). The differences in the membrane domains are responsible for the unique properties of each isozyme. Hmg1p is a stable protein with a half-life greater than 8 hours (Hampton and Rine, 1994). Hmg2p is an unstable protein with a half-life of 60 minutes and is known to be degraded by the proteasome (Hampton and Rine, 1994; Hampton *et al.*, 1996). Yeast cells respond differently to elevated levels of Hmg1p versus elevated levels of Hmg2p. Characteristic types of membrane proliferations are formed in *Saccharomyces cerevisiae*. Specifically, Hmg1p

triggers the formation of nuclear-associated membrane stacks called karmellae (Wright *et al.*, 1988). In contrast, Hmg2p induces peripheral ER membrane stacks and short karmellae (Koning *et al.*, 1996). Koning *et al.* demonstrated that Hmg1p and Hmg2p are localized to different ER subcompartments at elevated levels and that the protein composition of these compartments can be regulated. Specifically, Kar2p, the ER-lumenal chaperone, was excluded from Hmg2-type membrane proliferations but not from Hmg1-induced karmellae (Koning *et al.*, 1996).

Because yeast is a genetically malleable organism, we have chosen to study the signaling pathway that leads to karmellae biogenesis in *Saccharomyces cerevisiae.* Because many cell types perceive an increase in the level of HMG-CoA reductase as a signal for ER membrane biogenesis, what we learn from our studies in yeast will be applicable to membrane synthesis in other eukaryotes. Analysis of the karmellae-inducing signal will give us a molecular description of the first part of the pathway. Identification of new proteins that interact with HMGR will allow characterization of downstream components in this signaling pathway. New interacting proteins may also provide additional information concerning the regulation of HMGR. Because HMG-CoA reductase has a critical role in cholesterol production, these studies may have clinical applications as well. Analysis of karmellae biogenesis has the potential to reveal basic insights into the general principles for membrane assembly and organization.

Outline of work in this dissertation

The work described in Chapter 2 elucidates the contribution of cytosolic sequences on Hmg1p in order for Hmg1p to function as a karmellae-inducing signal.

We discovered that sequences at the carboxyl terminus of Hmg1p can profoundly affect the ability of the protein to induce karmellae. Specifically, truncations of Hmg1p that removed or shortened the cytosolic domain were unable to induce karmellae, even though the mutant protein accumulated to normal levels. This result indicated that the membrane domain of Hmg1p was not sufficient to signal for karmellae assembly. Using β–galactosidase fusion proteins, we demonstrated that the carboxyl terminus did not simply serve as an oligomerization domain. This chapter was submitted to *Molecular Biology of the Cell* in April 1999.

Chapter 3 describes the isolation and characterization of mutant *HMG1* alleles defective for karmellae biogenesis. To identify the critical amino acids for karmellae signaling, we introduced random point mutations into the Loop G-encoding portion of *HMG1*. We randomly mutagenized the Loop G sequence via mutagenic PCR, expressed the mutagenized Hmg1p in yeast, and screened for inability to generate karmellae. Out of 4,000 strains with Loop G mutations, we isolated 29 karmellae-defective Loop G-encoding regions. Therefore, less than 1% of Loop G mutations reduced the ability of the protein to induce karmellae. To test the mutant Loop G alleles for dominance, we examined karmellae assembly in a strain expressing the wild-type Hmg1p and a Loop G mutant Hmg1p. Karmellae assembly was restored to 75% of the wild-type level in a strain expressing both the wild-type Hmg1p and a mutant Hmg1p. Therefore, the mutant Loop G alleles are recessive to the wild-type *HMG1*. Sequencing the mutant Loop G regions demonstrated that mutations which reduced the ability of the protein to generate karmellae occurred in both conserved residues and in non-conserved residues. Analysis of Loop G sequences from karmellae-defective as well as karmellae-competent strains indicated that changes in charged residues led to a defect in karmellae

biogenesis. Our hypothesis is that Loop G serves as a karmellae-inducing signal by mediating protein-protein interactions and that the critical residues maintain the contact sites required to permit these interactions. This chapter will be submitted to *Yeast* in May 1999.

Figure 1.1 An overview of the mevalonate pathway highlighting the positions of HMG-CoA reductase and HMG-CoA synthase. Lovastatin is a competitive inhibitor of HMG-CoA reductase. Double arrows signify that there are subsequent steps which lead to the products shown.

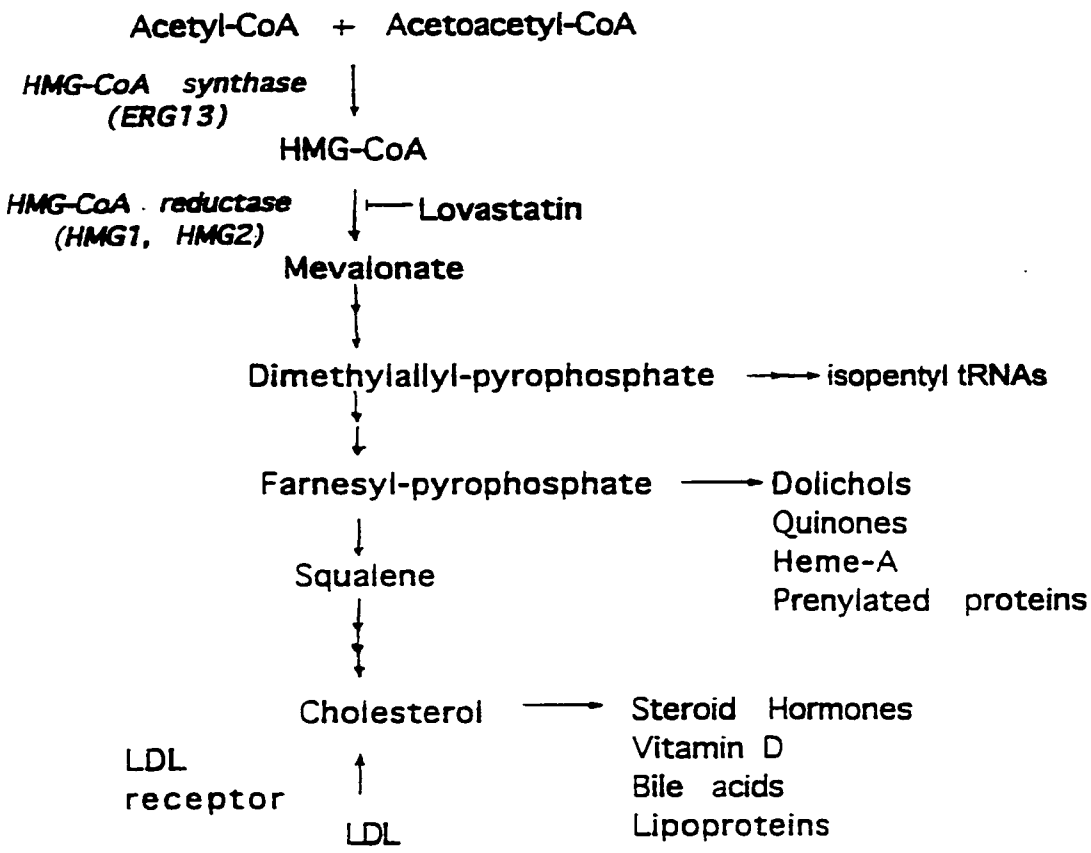
Acetyl-CoA + Acetoacetyl-CoA
HMG-CoA synthase (ERG13)
HMG-CoA
HMG-CoA reductase (HMG1, HMG2)
Lovastatin
Mevalonate
Dimethylallyl-pyrophosphate
isopentyl tRNAs
Farnesyl-pyrophosphate
Dolichols
Quinones
Heme-A
Prenylated proteins
Squalene
Cholesterol
Steroid Hormones
Vitamin D
Bile acids
Lipoproteins
LDL receptor
LDL

Chapter 2: The role of the cytosolic domain of HMG-CoA reductase in karmellae biogenesis

Abstract

In all cells examined, specific endoplasmic reticulum (ER) membrane arrays are induced in response to increased levels of the ER membrane protein, HMG-CoA reductase (HMGR). In yeast, expression of Hmg1p, one of the two yeast HMG-CoA reductase isozymes, induces assembly of nuclear-associated ER stacks called karmellae. Understanding the features of HMGR that signal karmellae biogenesis would provide useful insights into the regulation of membrane biogenesis. The HMGR protein consists of two domains, a polytopic membrane domain and a cytosolic catalytic domain. Experiments from our laboratory had indicated that the HMGR membrane domain was exclusively responsible for generation of ER membrane proliferations. Surprisingly, we discovered that this conclusion was incorrect: sequences at the carboxyl terminus of HMGR can profoundly affect karmellae biogenesis. Specifically, truncations of Hmg1p that removed or shortened the carboxyl terminus were unable to induce karmellae, even though the mutant protein accumulated to normal levels. This result indicated that the membrane domain of Hmg1p was not sufficient to signal for karmellae assembly. Using β–galactosidase fusion proteins, we demonstrated that the carboxyl terminus did not simply serve as an oligomerization domain. Our working hypothesis is that a truncated or misfolded cytosolic domain prevents proper signaling for karmellae biogenesis by interfering with the required tertiary structure of the membrane domain.

Assembly of specific membranes is an essential process throughout cell growth and development, but the molecular mechanisms responsible for specific membrane biogenesis are not known in even a single case. Specific ER membrane arrays are induced by increasing the levels of certain ER membrane proteins, such as HMG-CoA reductase (Wright *et al.*, 1988), cytochrome P450 (Schunck *et al.*, 1991), cytochrome b5 (Vergeres, *et al.*, 1993), ribosomal receptor (Wanker *et al.*, 1995) Sec12p (Nishikawa *et al.*, 1994), microsomal aldehyde dehydrogenase (Yamamoto *et al.*, 1996), and Pbn1p (Naik and Jones, 1998). Analysis of these inducible membranes provides an opportunity to discover the molecular mechanisms cells use to regulate the synthesis and organization of new membrane arrays.

HMG-CoA (3-hydroxy-3-methylglutaryl Coenzyme A) reductase is an integral ER membrane protein that catalyzes the production of mevalonate, a key intermediate in the synthesis of sterols and non-sterol isoprenoid compounds. The structure of HMG-CoA reductase can be divided into two domains, a complex membrane-spanning domain followed by a cytosolic catalytic domain (Basson *et al.*, 1988; Roitelman *et al.*, 1992). The amino-terminal half of mammalian and yeast HMGRs spans the membrane eight times and is connected to the catalytic domain through a linker sequence (Roitelman *et al.*, 1992; Lum *et al.*, 1996). The membrane domain is responsible for the proliferation of ER membranes (Jingami *et al.*, 1987; Parrish *et al.*, 1995) and the regulated degradation of both the mammalian and yeast HMGRs (Gil *et al.*, 1985; Skalnik *et al.*, 1988; Hampton and Rine, 1994). The cytosolic domain is responsible for catalysis and is thought to mediate protein dimerization (Frimpong *et al.*, 1994; Edwards *et al.*, 1985; Basson *et al.*, 1987).

Unlike mammalian cells, which have one HMG-CoA reductase, yeast express two functional HMGR isozymes, Hmg1p and Hmg2p (Basson *et al.*, 1986).

Each isozyme triggers the proliferation of distinct sets of membrane arrays that reflect the localization of the particular isozyme (Koning *et al.*, 1996). Specifically, Hmg1p triggers the formation of karmellae, which are stacked pairs of membranes associated with the nucleus (Wright *et al.*, 1988). Hmg2p induces peripheral ER membrane stacks and short karmellae(Koning *et al.*, 1996). The ability to respond to HMGR elevations by generating ER membrane arrays is not unique to yeast, but occurs in all cell types. For example, in mammalian cells, HMGR induces the formation of hexagonal arrays of smooth ER tubules called crystalloid ER (Chin *et al.*, 1982; Pathak *et al.*, 1986; Jingami *et al.*, 1987; Kochevar and Anderson, 1987).

Over the years our laboratory had made several observations using chimeric fusion proteins which indicated that the catalytic domain of HMGR played no role in either induction or morphology of membrane biogenesis. For example, proteins containing the HMGR membrane domain fused to unrelated carboxyl-terminal sequences such as Suc2His4Cp induced the proliferation of ER membrane arrays that were indistinguishable from the membranes generated by the wild-type HMGR (Parrish *et al.*, 1995). To determine if the membrane domain of Hmg1p was sufficient to induce karmellae, we generated truncations of Hmg1p that shortened or completely removed the carboxyl terminus. Surprisingly, although the truncated proteins were expresssed at high levels, yeast did not generate karmellae in response to them. Therefore, sequences beyond the membrane domain must be playing some role in the process of signaling for karmellae. One postulated role for the carboxyl-terminal sequences is to provide an oligomerization domain that would allow the reductase proteins to associate with each other. This hypothesis was tested by fusing the Hmg1p membrane domain to an oligomerization- competent β-galactosidase and to an oligomerization-incompetent truncated β-galactosidase (Fowler and Zabin, 1983). Both β-galactosidase chimeras induced karmellae, indicating that oligomerization of the cytosolic domain was not a

requirement. Our experiments suggested that the carboxyl terminus of HMGR was not neutral for karmellae assembly and that the role of the cytosolic domain was unlikely to be oligomerization.

Materials and Methods

Strains and Media

The yeast strains used in this study are listed in Table 2.1. Strains were grown at 30°C on rich minimal medium (0.67% yeast nitrogen base without amino acids, 2% casamino acids, and 2% glucose or 2% galactose plus 3% sucrose) supplemented with the appropriate acids or nucleotide bases (Sherman *et al.*, 1986) or complete synthetic medium (CSM) minus histidine minus uracil from Bio 101 (La Jolla, CA). Solid medium contained 2% agar (Sherman *et al.*, 1986).

Plasmids

To truncate Hmg1p after the membrane domain, pCS4-14, a derivative of pCS4 with an XhoI site immediately after the membrane domain coding region (Sengstag *et al.*, 1990) was digested with *XhoI* and *ClaI* to add a synthetic double-stranded oligonucleotide with the HA epitope and a stop codon, resulting in plasmid pDP428. The HA epitope is a nonapeptide sequence derived from the influenza hemagluttin protein (Wilson *et al.*, 1984). This plasmid encodes the N-terminal 523 amino acids of Hmg1p (the entire membrane domain), followed by 14 amino acids that included the HA epitope and a stop codon. The double stranded oligonucleotide was prepared by annealing the following oligonucleotides: 5'TCGAGCATACCAGTTACCCATACGATGTTCCAGATTACGCTTAACTAGTT GA 3' and 5'CGTCAACTAGTTAAGCGTAATCTGGAACATCGTATGGGTAACTG

GTATGC 3'.

To create Hmg1:β-galactosdiase fusion proteins, pDP428 was digested with *XhoI* and*SpeI* to insert an *XhoI-SpeI* fragment containing wildtype *lacZ* (pDP598) or to insert an *XhoI-SpeI* fragment containing a truncated *lacZ* (pDP600). The full-length β-galactosidase was obtained from the plasmid pMKITNeo-*XhoI*-HMGalδ5', and the truncated β-galactosidase was obtained from the plasmid pMKITNeo-*XhoI*-HMGalδ20 (both provided by Helen Cheng and Robert Simoni, Stanford University, Palo Alto, CA). These plasmids contain Syrian hamster HMGR fused to β-galactosidase or a truncated β-galactosidase with the last 20 amino acids removed. Both intermediate plasmids, pDP598 and pDP600, needed a correction in reading frame in order to encode the N-terminal 523 amino acids of Hmg1p, followed by 76 amino acids of Syrian hamster HMGR linker region, and then ending with the entire β-galactosidase or β-galactosidase missing the last 20 amino acids. The reading frame between the Hmg1p membrane domain and the hamster HMGR linker region was corrected by inserting a double-stranded oligonucleotide. The double-stranded oligonucleotide was prepared by annealing two oligonucleotides: 5'TCGAACATACCAGTACG3' and 5'TCGACGTACTGGTATGT 3'. The final plasmids are pDP601 with the full-length β-galactosidase fusion and pDP602 with the truncated β-galactosidase fusion Δ20.

The galactose-inducible HMGR plasmid pGAL-*HMG1* (pAK266) has been previously described (Koning *et al.*, 1996). To create a catalytically inactive HMGR mutant, pAK266 was digested with *KpnI* and then religated. This plasmid (pAK260) encodes the *GAL1/10* promoter, N-terminal 987 amino acids of Hmg1p (which includes the entire membrane domain and most of the catalytic domain), followed by a 29 amino acid gap, and then the remaining 68 amino acids of Hmg1p. The green fluorescent protein (GFP; (Prasher *et al.*, 1992; Chalfie *et al.*, 1994)) expression constructs used in these studies were derived from the plasmid pJC81

(provided by Jeff Cox and Peter Walter, UCSF, San Francisco, CA). This plasmid contains a mutant version of *GFP10* in which the first two codons have been changed to encode a *Bam*HI site. To create a membrane domain Hmg1:GFP fusion, a 1.5 kb *Bam*HI-*EagI* fragment of pJC81 (containing the 710 bp *GFP10* open reading frame, 400 bp of the *ACT1* gene containing the transcriptional terminator, and 390 bp of the *tet* gene) was subcloned into the *Bam*HI-*EagI* sites of pRS316 (Sikorski and Hieter, 1989), creating plasmid pCR415. This plasmid, pCR415, was then digested with *BamHI* and *SmaI*, treated with Klenow to fill in the ends and religated, creating pCR426. A 2.2 kb *EcoRI* fragment containing pGAL-HMG1 from pJR435 (Basson *et al.*, 1988) was ligated into the *EcoRI* site of pCR426, creating plasmid pCR427. This plasmid encodes an $Hmg1^{mem}$:GFP fusion, consisting of the *GAL1/10* promoter, N-terminal 525 amino acids of Hmg1p, followed by three linker residues and all of GFP except the initiating methionine. The cytosolic Hmg1:GFP fusion encoded by pCR425 has been previously described (Koning *et al.*, 1996). This plasmid encodes the *GAL1/10* promoter, N-terminal 987 amino acids of Hmg1p, followed by two linker residues and all of GFP except the initiating methionine.

To exchange the Hmg1p catalytic domain with the catalytic domain of Hmg2p, pA7, which contains an introduced *XhoI* site after the sequences encoding the Hmg1p last transmembrane domain (Sengstag *et al.*, 1991) was digested with *HindIII*, treated with Klenow, and then cut with *XhoI*. The resulting 9 kb fragment contained the *HMG1* promoter and all the membrane domain coding sequences as well as vector sequences. A 2 kb fragment that contains the Hmg2p linker region and catalytic domain coding sequences was isolated from pB7, which contains an introduced *SalI* site after the last transmembrane domain of Hmg2p (Sengstag *et al.*, 1991). This fragment was isolated after digestion with *EcoRI*, treatment with Klenow, and then digested with *SalI*.

Ligation of the fragments produced pCS40, which encodes the *HMG1* promoter, N-terminal 525 amino acids of Hmg1p, fused to the Hmg2p linker and catalytic domain.

The multicopy (2 micron) plasmid, pRH127-3, which expressed the soluble Hmg1p catalytic domain under the control of the constitutive *GAPDH* promoter, has been previously described (Donald *et al.*, 1997). To co-express full-length Hmg1p with the soluble Hmg1p catalytic domain, a galactose-inducible *HMG1* plasmid, pAK266, was digested with *XhoI* and *SpeI* yielding a 4.3 kb fragment with the *GAL1/10* promoter and *HMG1*. This fragment was ligated into the *XhoI*, *SpeI* sites of pRS313 (Sikorski and Hieter, 1989) to produce a *CEN-GAL1/10-HMG1* plasmid in a vector that contains the *HIS3* selectable marker (pDP586).

$DiOC_6$ Staining

$DiOC_6$ (3,3'-dihexyloxacarbocyanine iodide) staining was performed as previously described (Koning *et al.*, 1993). Cells in log phase of growth were stained with 10μg/ml $DiOC_6$ (Kodak, Rochester, NY) per 10^7 cells using a 1 mg/ml ethanolic stock. Stained cells were observed with conventional fluorescence optics, using a Nikon Microphot-FXA epifluorescence microscope with excitation (480+/-20nm) and barrier (535+/40nm) filters appropriate for fluorescein.

Electron Microscopy

Preparation of cells for electron microscopy was a variation on methods previously described (Wright and Rine, 1989). Specifically, cells were grown to 1 OD_{600}/ml and the culture was fixed in 2% glutaraldehyde in buffer (0.1 M PIPES pH 6.8, 1mM $CaCl_2$, 1mM $MgCl_2$), then postfixed in 2% $KMnO_4$, and stained *en bloc* with 1% uranyl acetate. The cells were dehydrated through a graded ethanol series, and embedded in Spurr's resin (Spurr, 1969). Sections were stained with Reynold's lead

citrate (Reynolds, 1963). Observations were made on a Phillips 100 CMT microscope at 60-80 kV.

Immunofluorescence

Immunofluorescence was performed using a procedure similar to that described (Pringle *et al.*, 1983). Log phase cells were fixed with 3.7% formaldehyde, treated with Zymolyase (United States Biological, Swampscott, MA) to partially remove their cell walls, and applied to multiwell slides (Koning *et al.*, 1996). Antisera generated against the carboxyl terminal 15 amino acids of Hmg1p (LDII) was used at a 1:100 dilution. Kar2p antibodies were a gift of Mark Rose (Princeton University, Princeton,NJ) and were used at a 1:2000 dilution. GFP antibody was purchased from Clontech (Palo Alto, CA) and used at a 1:100 dilution. HA antisera (12CA5) was purchased from Boehringer Mannheim Biochemica (Indianapolis, IN) and used at a 1:100 dilution. A 1:800 dilution of rabbit anti-βgalactosidase antibody (Cappel Organon Technika, Durham, NC) was used. Previously, the anti-βgal serum was pretreated by incubation with a cellular lysate from fixed, glass-bead lysed yeast. In all cases, the incubation in primary antisera was for 1 hour at room temperature. The antibody solution was gently aspirated away and the cells were washed 5 times with TBST (25mM Trizma base, 3mM KCl, 140mM NaCl, 0.05% Tween-20). Then 10 µl of blocking solution (TBST+1% ovalbumin) was applied to each well. In all cases, 10 µl of secondary antibody was diluted in blocking solution, centrifuged for 10 min at 12,000 rpm in a microcentrifuge, and applied to the appropriate wells. The secondary antibodies used were: 1:1000 Goat anti-rabbit fluorescein conjugated; 1:200 Goat anti-mouse fluorescein conjugated; or 1:500 Goat anti-rabbit Texas red conjugated, Cappel Organon Technkia, Durham, NC. After 45 minutes, the secondary antibody was washed with TBST 5 times. 10 µl of a 1:1000 dilution of 1mg/ml DAPI (Sigma, St.

Louis, MO) in TBS was added to each well for 1 minute. After one rinse with TBS, a drop of Citifluor (Ted Pella, Redding, CA) was applied to each well, and the slide sealed with a coverslip and nailpolish. Each experiment included a positive control using an antibody to detect tubulin (Yol1/34 (1:10 dilution) Accurate Chemical and Scientific Company, Westbury, NY) and a negative control lacking primary antiserum.

Protein Preparation and Immunoblotting

After growth in galactose for 12 hours, the cultures were diluted into fresh medium (YM CAA 2% galactose, 3% sucrose) and grown for 4 to 6 hours until they reached 1 OD600/ml. A 16-18 hour galactose induction was used because a high level of karmellae is observed in cells after 12 hours in galactose. The cells were then pelleted for 5 min at 834 x g in a clinical centrifuge, and the cell pellets were frozen at -80oC until lysed. Strains that did not contain galactose-inducible plasmids were grown overnight in YM CAA 2% glucose medium. The next morning, the cells were diluted into fresh glucose medium and grown to 1 OD600/ml before harvesting a cell pellet. A total membrane fraction was prepared from the cells using modifications of previously described methods (Deschenes and Broach, 1987; Koning *et al.*, 1996). The pelleted membranes were resuspended in 100 µl lysis buffer (0.3M sorbitol, 0.1M NaCl, 5mM MgCl2, 20mM MOPS pH 7.4) containing protease inhibitors (2µg/ml each TPCK (N-tosyl-L-phenylalanine-chloromethyl ketone), leupeptin, pepstatin A, aprotinin) found in complete tablets (Boehringer Mannheim Biochemica, Indianapolis, IN). The absorbance at 280 nm was measured for each sample in 1% SDS, and 100 A_{280} units were loaded on duplicate gels after heating at 65^{0}C in 1X Laemmli sample buffer (0.03M Tris-HCl, pH 6.8, 2% SDS, 10% glycerol, 5% β-mercaptoethanol, 0.005% Bromophenol blue) for 10 min followed by a 5 min centrifugation at top speed in a microcentrifuge (Laemmli, 1970). One gel was blotted to nitrocellulose and processed

for immunodetection as described (Lum and Wright, 1995), and the duplicate gel was stained with Colloidal blue from Novex (San Diego, CA). The duplicate gel and Western blot were digitized by scanning and analyzed using NIH Image 1.60 software as described (Lum and Wright, 1995). The above membrane preparation procedure was used to determine the stability of the entire Hmg1p or Hmg1 fusion protein pool by measuring the relative amount of Hmg1p immunoreactivity remaining at various timepoints after blocking protein synthesis with 50 μg/ml cycloheximide (CHX) (Hampton and Rine, 1994).

β-galactosidase Activity Assays

The strains, RWY 943 and RWY 944 were assayed for β-galactosidase activity according to the protocol of Guarente (Guarente, 1983). Briefly, log phase cells were resuspended in buffer, SDS, and chloroform. Then o-Nitrophenyl-β–D–galactoside (ONPG) was added as the substrate for β-galactosidase. The reaction was stopped by adding Na_2CO_3, and the cell debris was removed by centrifugation. The OD_{420} was measured, and the results were normalized to the OD_{600} of the culture and to the assay time. Duplicate assays were run in each case and cell dilutions were determined to be in the linear range of the assay.

Results

Truncating the Hmg1p carboxyl terminus reduced or eliminated the protein's ability to induce karmellae.

Yeast cells respond to increased levels of Hmg1p by proliferating stacked pairs of nuclear-associated membranes called karmellae (Wright *et al.*, 1988). To determine if the cytosolic domain of Hmg1p was required for karmellae biogenesis, we

examined the organization of the ER in cells expressing wild-type or truncated Hmg1p proteins by fluorescence microscopy (summarized in Figure 2.1) and electron microscopy (Figure 2.2). In this study, Hmg1p levels were elevated by use of either a galactose-inducible promoter or a multicopy plasmid, resulting in approximately a ten-fold increase in protein in both cases. As expected, karmellae were observed in 35% of the cells expressing wild-type Hmg1p (Figure 2.2A). Note that karmellae are never observed in 100% of the cell population in part because karmellae remain in the mother cell at mitosis (Wright *et al.*, 1988). Surprisingly, the truncated Hmg1p that lacked a catalytic domain (Hmg1 ^{mem}:HA) failed to induce karmellae or any other type of ER membrane proliferation (Figure 2.2B).

We considered the possibility that removal of the entire catalytic domain might have profound effects on the folding of the Hmg1p membrane domain. If so, less dramatic changes to the catalytic domain should allow the protein to remain karmellae competent. To test this idea, we examined the ultrastructure of cells expressing a catalytically inactive Hmg1p missing only 29 amino acids within the catalytic domain (Hmg1Δ29p) and determined that only 1% of the cell population contained karmellae (Figure 2.2C). In an additional 1% of the cell population, the Hmg1Δ29p induced tubular ER stacks, which resembled the mammalian crystalloid ER (Figure 2.2D). This dramatic reduction in karmellae was unexpected since the catalytic domain can be completely replaced with unrelated carboxyl-terminal sequences without adversely affecting the ability of the protein to induce karmellae (Parrish *et al.*, 1995). In addition, we had previously confirmed that catalytic activity of Hmg1p was not required for karmellae biogenesis by examining the ultrastructure of cells expressing a catalytically inactive allele of *HMG1* in which a single amino acid had been changed and demonstrating that this mutant Hmg1p induced karmellae to the wild-type level (Profant, unpublished observations). Thus, neither a specific protein sequence or activity

appeared to be necessary for ability to induce karmellae, yet even rather minor changes to the Hmg1p carboxyl terminus could interfere with karmellae assembly.

We also examined cells expressing an Hmg1 membrane:Hmg2 catalytic domain fusion, in which the Hmg2p catalytic domain replaced the Hmg1p catalytic domain ($Hmg1^{mem}$:$Hmg2^{cat}$). We predicted that $Hmg1^{mem}$:$Hmg2^{cat}$ will generate karmellae because the information in the Hmg1p membrane domain is postulated to dictate the cell's response. In addition, the catalytic domain is highly conserved between Hmg1p and Hmg2p (Basson *et al.*, 1988). As expected, the $Hmg1^{mem}$:$Hmg2^{cat}$ induced predominantly karmellae (Figure 2.2H). However, in 4% of the cell population, the $Hmg1^{mem}$:$Hmg2^{cat}$ induced Hmg2-type membranes. Therefore, information present in the Hmg2 catalytic domain continued to exert some influence on the membranes generated even in the context of the Hmg1p membrane domain.

To further investigate the role of carboxyl-terminal sequences in karmellae biogenesis, we characterized the membrane proliferations induced by two different Hmg1:GFP fusion proteins. The first fusion included a portion of the Hmg1p catalytic domain ($Hmg1^{mem}$:$Hmg1^{525-987}$:GFP). In the second fusion, the cytosolic domain of Hmg1p was completely replaced by GFP ($Hmg1^{mem}$:GFP). Karmellae were induced by $Hmg1^{mem}$:$Hmg1^{525-987}$:GFP (Figure 2.2G). In contrast, as for the $Hmg1^{mem}$:HA protein, karmellae were never observed in cells expressing $Hmg1^{mem}$:GFP;.instead 10% of the cells assembled disorganized ER membrane stacks (Figure 2.2E and 2.2F). The disorganized ER consisted of either portions of the nuclear envelope folding away from the nucleus or peripheral membrane stacks. These observations are consistent with an essential, but unexpected, role for the carboxyl terminus in karmellae biogenesis.

Differences in protein amounts did not account for the inablility to induce karmellae.

Elevated levels of Hmg1p are required to induce karmellae (Wright *et al.*, 1988). Thus, mutations that decrease the amount of Hmg1p would be unable to induce karmellae assembly. We determined that the steady-state levels of all of the fusion proteins were 70-94% of wild-type, verifying that adequate protein was expressed to induce karmellae assembly in each case (Figure 2.3).

An alternate explanation for the inability of certain *HMG1* constructs to generate karmellae is that Hmg1p fusion proteins that cannot induce karmellae may have decreased stabilities. To investigate this possibility, we compared levels of Hmg1p that remain following addition of cycloheximide. Because cycloheximide inhibits new protein synthesis, the amount of protein remaining at various times after treatment can be used to assess the degradation rate of the protein in question (Hampton and Rine, 1994). As expected (Hampton and Rine, 1994), wild-type Hmg1p was stable, with little degradation observed after 4 hours of cycloheximide treatment (Figure 2.4A). The truncated Hmg1p that lacked a cytosolic domain (Hmg1^{mem}:HA) (Figure 2.4B) and the Hmg1Δ29p (Figure 2.4D) were also stable after 4 hours of cycloheximide treatment. In addition, both the Hmg1^{mem}:GFP protein (Figure 2.4C) and the Hmg1^{mem}:Hmg1$^{525-987}$:GFP protein (Figure 2.4E) were stable after 4 hours in cycloheximide. In contrast to Hmg1p, intact Hmg2p is quite unstable, with a half-life of 60 minutes (Hampton and Rine, 1994). Unlike wild-type Hmg2p, Hmg1^{mem}:Hmg2^{cat} protein was stable after 4 hours of cycloheximide treatment (Figure 2.4E) confirming previous data which led to the idea that the membrane domain of the protein determines its half-life (Gil *et al.*, 1985; Skalnik *et al.*, 1988; Hampton and Rine, 1994). In Figure 2.4E, the percent decrease in protein after 4 hours was plotted for the different Hmg1p fusions, showing that the fusion proteins had similar stabilities. These results eliminated the possibility that the fusions were unable to signal for karmellae due to inadequate steady-state protein levels or to instability of the Hmg1p variants.

Alteration of the cytosolic domain of Hmg1p did not cause mislocalization of the protein to the peripheral ER.

The ability of a protein to induce karmellae might depend upon its specific localization within the cell (Koning *et al.*, 1996) Since karmellae arise from the nuclear envelope, a protein capable of signaling for karmellae assembly would be expected to be localized in the nuclear envelope. Consistent with this hypothesis, increased levels of wild-type Hmg1p are present predominantly in the nuclear envelope; in contrast, increased levels of Hmg2p localize predominantly to the peripheral ER (Koning *et al.*, 1996).

The subcellular localization of the fusion proteins was examined by immunofluorescence to assess whether alterations in the cytosolic domain of Hmg1p influenced the distribution of the protein within the ER. As expected, wild-type Hmg1p was present predominantly in the nuclear envelope, with increased fluorescence found in cells generating karmellae (Figure 2.5, A and B). The localization of the lumenal ER protein, Kar2p, demonstrates the pattern for proteins found throughout the ER (Rose *et al.*, 1989; Preuss *et al.*, 1991). In Figure 2.5C and 2.5D, Kar2p staining appeared in the nuclear envelope and in a network stretching to the cell periphery. The Hmg1Δ29p had a localization pattern indistinguishable from wild-type Hmg1p (Figure 2.5, E and F), indicating that the inability of this protein to generate karmellae was not due to an altered distribution within the ER. The localization pattern for Kar2p in the strain expressing Hmg1Δ29p was unaltered from wild-type Kar2p localization (Figure 2.5, G and H).

In Figure 2.6, the truncated Hmg1p lacking a catalytic domain ($Hmg1^{mem}$:HA) was localized using a monoclonal antibody (12CA5) to the HA epitope. Although the staining pattern was less distinct in these cells, the protein was detected in

the nuclear envelope and in the ER network extending throughout the cytosol. Most of the cells exhibited nuclear envelope staining in a ring surrounding the nucleus (Figure 2.6, A and B). Thus, the truncated Hmg1^{mem}:HA protein appeared to be localized throughout the ER instead of displaying a predominantly nuclear envelope pattern. The Kar2p localization pattern is shown for comparison in Figure 2.6C and 2.6D. To confirm the specificity of the HA antibody, immunofluorescence was performed on a yeast strain that was not expressing a HA-tagged protein. No immunofluorescence patttern was observed in these cells, but the entire cell was faintly visible (data not shown).

Next, we investigated the localization patterns of the two Hmg1:GFP fusions. The Hmg1^{mem}:Hmg1$^{525-987}$:GFP protein, which generates karmellae, was localized in the nuclear envelope (Figure 2.7, E and F and Koning *et al.*, 1996) similar to wild-type Hmg1p. The Hmg1^{mem}:GFP fusion, which failed to generate karmellae, had a nuclear envelope localization pattern with some peripheral ER staining (Figure 2.7, A and B) again appearing similar to that of wild-type Hmg1p.

Taken together, the localization patterns demonstrated that the failure to assemble karmellae in response to the Hmg1p fusions was not due to a large proportion of the protein being mislocalized out of the ER or mislocalized exclusively to the peripheral ER. However, from our data we cannot rule out the possibility that subtle alterations in the localization of the protein, such as that observed for the Hmg1^{mem}:HA, might influence the ability of the protein to induce karmellae.

Competition with the soluble catalytic domain reduced the overall level of karmellae generated by the wild-type Hmg1p.

Our results suggested that the membrane domain and the cytosolic domain of Hmg1p cooperate in some way to generate karmellae. To test this idea, we examined

karmellae assembly in a strain expressing both the full-length Hmg1p and a truncated protein containing only the linker and the catalytic domain of Hmg1p. Since HMGR is thought to act as a dimer using contact sites in the catalytic domain (Frimpong *et al.*, 1994; Edwards *et al.*, 1985; Basson *et al.*, 1987), we hypothesized that expression of a soluble catalytic domain would interfere with the ability of the holoprotein to dimerize and to induce karmellae. It is important to note that the catalytic domain is capable of proper folding and oligomerization in the absence of attachment to the membrane domain since it is enzymatically active and the amount of activity parallels the protein amount (Donald *et al.*, 1997) As expected, elevated expression of the soluble catalytic domain alone was incapable of inducing karmellae (Table 2.2). In the strain expressing both the holoprotein and the soluble catalytic domain, the soluble Hmg1p catalytic domain was expressed at three-fold higher levels than the holoprotein (Table 2.2). In addition, the amount of Hmg1p holoprotein was not decreased relative to that seen in strains that are not simultaneously expressing the catalytic domain. Consequently by the law of mass action, and assuming that the proteins dimerized via carboxyl-terminal sequences, we expected that 86% of the holoprotein would be complexed with a soluble catalytic domain and that 14% of the holoprotein would form holoprotein-holoprotein dimers. Thus, if dimerization between holoproteins were important for karmellae assembly, a dramatic drop in the level of karmellae should be seen. Specifically, we would predict that the proportion of cells containing karmellae should decrease from 41% to less than 6% (an 85% decrease). Unexpectedly, karmellae assembly was decreased by only 33% in the strain expressing both the holoprotein and the soluble catalytic domain (Table 2.2). This result suggested that carboxyl-terminus mediated dimerization between holoproteins may not be essential for karmellae assembly.

Oligomerization of the cytosolic domain of Hmg1p was not required for karmellae formation.

To further test the hypothesis that oligomerization via the cytosolic domain was not required for karmellae assembly, we fused the Hmg1p membrane domain to β-galactosidase (β-gal) or to a truncated β-galactosidase missing the last 20 amino acids (β-galΔ20). Full-length β-galactosidase forms tetramers, which are the enzymatically active form of the enzyme; dimers and monomers are not catalytically active (Fowler *et al.*, 1983). Truncated β- galactosidase missing the last 10 amino acids is found as a monomer (Fowler *et al.*, 1983). In addition, β-galactosidase missing the last 16 amino acids lacks enzyme activity and runs on a nondenaturing gel as a monomer (Tsuneoka *et al.*, 1991). Although we did not directly assess the oligomerization state of either β-galactosidase fusion, the lack of β-galactosidase activity (Table 2.3) exhibited by $Hmg1^{mem}$: β-galΔ20 was consistent with this carboxyl-terminus being monomeric. Additionally, because $Hmg1^{mem}$: β-gal was enzymatically active (Table 2.3), we would argue that the carboxyl-termini of separate fusion proteins were capable of forming tetramers. If oligomerization of the cytosolic region on Hmg1p is critical for karmellae induction, then the $Hmg1^{mem}$:β-galΔ20 will fail to induce karmellae.

We performed immunoblots to measure expression of the β-galactosidase fusion proteins and to confirm the stability of the proteins. $Hmg1^{mem}$:β-gal was present at 85% and $Hmg1^{mem}$:β-galΔ20 was present at 81% of the wild-type Hmg1p steady-state protein level (Figure 2.3), and both fusions were stable during the 4-hour treatment with cycloheximide (Figure 2.8). Both $Hmg1^{mem}$:β-gal and $Hmg1^{mem}$:β-galΔ20 generated karmellae (Figure 2.9) and were localized predominantly to the nuclear envelope of the ER (Figure 2.10). Because $Hmg1^{mem}$:β-galΔ20 induced karmellae, oligomerization of the cytosolic domain did not appear to be required for karmellae signaling. However, cells expressing the $Hmg1^{mem}$:β-gal generated a higher level of

karmellae compared to cells expressing the Hmg1^{mem}:β-galΔ20 (Table 2.3). Interestingly, over time, the amount of karmellae in both strains increased.

Discussion

To explore how cells regulate the synthesis and organization of new membrane arrays, we studied the features of Hmg1p that are necessary for the protein to act as a signal for karmellae biogenesis. An earlier study with heterologous carboxyl-terminal fusions to HMG-CoA reductase suggested that the ability to induce membranes resides solely with the HMG-CoA reductase membrane domain (Parrish *et al.*, 1995). Our laboratory refined this result, identifying the last ER-lumenal loop within the Hmg1p membrane domain (Loop G) as a region that is critical for karmellae biogenesis (Parrish, *et al.*, 1995). Thus, it was surprising to discover that sequences at the carboxyl terminus could profoundly affect the ability of Hmg1p to induce karmellae.

When taken as a whole, results from this study make it unlikely that the inability of certain Hmg1p constructs to induce karmellae reflects mislocalization of the protein, an insufficient level of protein, an unstable protein, or the inability to oligomerize via the carboxyl terminus. Instead, we propose that the karmellae biogenesis defects result from alterations of the carboxyl terminus that perturb the conformation of the membrane domain. In support of the importance of the tertiary structure of the membrane domain for HMG-CoA reductase signaling, deletion of two contiguous membrane-spanning regions in hamster HMG-CoA reductase resulted in a protein that did not induce crystalloid ER; but instead induced disordered sheets of ER (Jingami *et al.*, 1987).

Earlier studies designed to identify the critical features of protein that can induce ER proliferations emphasized the role of oligomerization at cytosolic domain interfaces (Gong *et al.*, 1996; Yamamoto *et al.*, 1996). For example, microsomal

aldehyde dehydrogenase (msALDH) can induce crystalloid ER similar to that induced by HMG-CoA reductase (Yamamoto *et al.*, 1996). msALDH has a single transmembrane domain and a large cytosolic domain, both of which are required for crystalloid ER induction. These authors postulate that organization of the crystalloid ER stems from interactions between the large cytosolic domains of msALDH in adjacent membranes (Yamamoto *et al.*, 1996). Extending this idea to Hmg1p, interactions between cytosolic domains would be responsible for organizing the karmellae into stacks and thereby determine the type of ER proliferation. Our results do not support a requirement for cytosolic oligomerization because the $Hmg1^{mem}$:β-galΔ20 generated karmellae (Figure 2.9). However, since $Hmg1^{mem}$:β-galΔ20 generated lower levels of karmellae that increased with time (Table 2.3), oligomerization at the carboxyl terminus may aid in clustering membrane domains which increases the local concentration of the Hmg1p signaling molecules.

Our results from the competition experiment in which the soluble catalytic domain of Hmg1p and the Hmg1p holoprotein are co-expressed also suggest that lateral clustering of membrane domains may be a prerequisite for karmellae signaling. As shown in Table 2.2, the strain expressing both the holoprotein and the soluble catalytic domain generated 67% of the wild-type karmellae level. We hypothesize that the moderate decrease in karmellae reflects complexes between a holoprotein and a soluble Hmg1p, which prevent the close lateral association between two membrane domains. In other words, the soluble Hmg1p is titrating away a portion of the membrane-bound Hmg1p thus decreasing potential associations between membrane-bound forms of Hmg1p. Thus, our data are consistent with the idea that Hmg1p membrane domain interactions are critical for communicating the need for ER proliferation.

Recently, another view that emphasizes protein quality has emerged to explain different types of ER proliferations that occur in response to mutant and wild-type cytochrome P450s. When expressed in *S. cerevisiae*, a wild-type cytochrome P450 of *Candida maltosa* generates tubular stacks of ER throughout the cytoplasm that appear distinct from karmellae (Zimmer *et al.*, 1997). In contrast, mutant forms of *Candida maltosa* cytochrome P450 expressed in *S. cerevisiae* lead to the proliferation of karmellae-like structures (Zimmer *et al.*, 1997). Because the mutant P450 forms have lower protein stability than the wild-type P450 enzymes, these authors favor a model in which a quality control system sorts the mutant P450 forms into a stacked ER subcompartment for degradation rather than the subcompartment responsible for tubular expansion (Zimmer *et al.*, 1997).

In our study, the Hmg1p variants which failed to induce karmellae did not have lower protein stabilities than the wild-type Hmg1p, making it unlikely that karmellae are assembled as degradative compartments to remove unstable proteins. Instead, these proteins may have other altered properties that distinguish them from a protein capable of inducing karmellae. We propose that these differences result in sorting of these proteins into different ER subcompartments. Consistent with this idea, when expressed at elevated levels, Hmg1p and Hmg2p are localized in different ER subcompartments that can have unique protein compositions (Koning *et al.*, 1996). For example, Kar2p, the ER-lumenal chaperone, is excluded from Hmg2-type membrane proliferations but not from Hmg1-induced karmellae (Koning *et al.*, 1996).

Our working model for karmellae signaling is that individual Hmg1p proteins transiently associate with one another via their membrane domains. Interactions between the attached catalytic domains also occur, but these interactions are not the key events needed for karmellae assembly. When the levels of Hmg1p are sufficiently high, stable complexes form that result in concentration of associated lipids or proteins into an

ER subdomain. This localized alteration in membrane composition activates the signaling pathway that ultimately leads to ER proliferation. We hypothesize that proper folding of the Hmg1p membrane domain is a critical first step in the karmellae signaling process, and that this folding can be influenced by sequences at the carboxyl terminus. In addition, sequences within the membrane domain itself, particularly Loop G, can affect interactions between Hmg1p membrane domains, thus influencing the formation and stability of the ER subdomain. Direct tests of this model will be challenging and will ultimately require sophisticated biophysical analyses. In the interim, additional work aimed at identifying proteins that interact with HMG-CoA reductase may provide important clues concerning the molecular events in the karmellae signaling process.

Table 2.1 Yeast strains and plasmids

Strain	Genotype
JRY527[a]	*MATa ade2-101 his3Δ200 lys2-801 met ura3-52*
RWY410[b]	JRY527 + pAK266
RWY406	JRY527 + pAK260
RWY614	JRY527 + pDP428
RWY572	JRY527 + pCS40
RWY621[b]	JRY527 + pCR425
RWY626	JRY527 + pCR427
RWY900	JRY527 + pRH127-3
RWY1494	JRY527 + pDP586
RWY1497	JRY527 + pDP586 + pRH127-3
RWY943	JRY527 + pDP601
RWY944	JRY527 + pDP602

Plasmid	Description
pAK266[b]	*pGAL:Hmg1p* in pRS316; *CEN6 URA3*
pAK260	*pGAL:Hmg1Δ29p* in pRS316
pDP428	*pHMG1: Hmg1^{mem}:HA* in YEp352; 2 micron origin *URA3*
pCS40	*pHMG1: Hmg1^{mem}:Hmg2 ^{cat}* in YEp352
pCR425[b]	*pGAL:Hmg1^{mem}:HMG1$^{525-987}$:GFP* in pRS316
pCR427	*pGAL: Hmg1^{mem}:GFP* in pRS316
pRH127-3[c]	*pGAPDH:Hmg1p catalytic* in Yplac195; 2 micron *URA3*
pDP586	*pGAL:Hmg1p* in pRS313; *CEN6 HIS3*
pDP601	*pHMG1:Hmg1:β-galactosidase* in YEp352
pDP602	*pHMG1:Hmg1:β-galΔ20* in YEp352

[a] Basson *et al.*, 1986

[b] Koning *et al.*, 1996

[c] Donald *et al.*, 1997

Figure 2.1 Summary of karmellae levels in cells expressing wild-type Hmg1p or the different Hmg1p fusion proteins. The fusion proteins used in this study are diagrammed together with the percentage of karmellae observed for the strains expressing each protein. These karmellae percentages were determined by scoring cells from three independent experiments. At least 400 cells were scored per experiment.

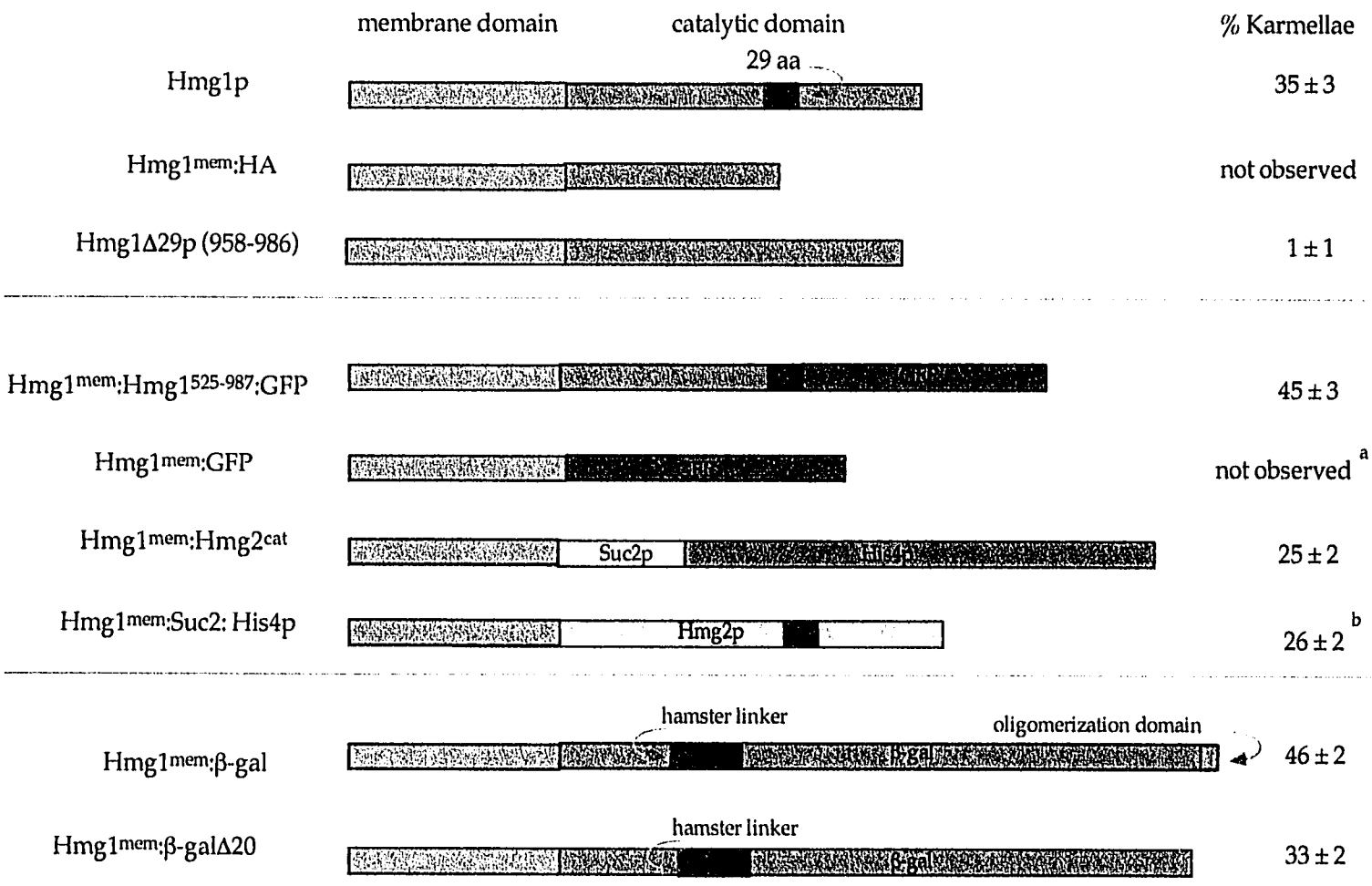

[a] 10% ± 1 altered ER proliferations

[b] 4% ± 1 Hmg2-type membranes

Figure 2.2 Truncating the carboxyl terminus of Hmg1p reduced the ability of the protein to induce karmellae. The ultrastructure of the nuclear envelope in a wild-type strain and in strains expressing the Hmg1p fusion proteins was compared. (A) A wild-type strain expressing intact Hmg1p (RWY 410) contains karmellae membranes in an ordered array on the nucleus. (B) Cells expressing the truncated Hmg1^{mem}:HA protein (RWY 614) lack any ER membrane proliferations. (C and D) Cells expressing the Hmg1Δ29p (RWY 406) usually lack karmellae (C) and sometimes produce extended ER networks (D). (E and F) Cells expressing the Hmg1^{mem}:GFP (RWY 626) do not generate karmellae but have altered ER arrays. (G) Cells expressing the Hmg1^{mem}:Hmg1$^{525-987}$:GFP (RWY 621) generate karmellae. (H) Cells expressing the Hmg1^{mem}:Hmg2 ^{cat} (RWY 572) generate karmellae predominantly. Occasionally, Hmg2-type membranes are found in the population of cells expressing the Hmg1^{mem}:Hmg2 ^{cat}. Arrows point to karmellae; arrowheads point to proliferated ER. Bars, 0.5 μm.

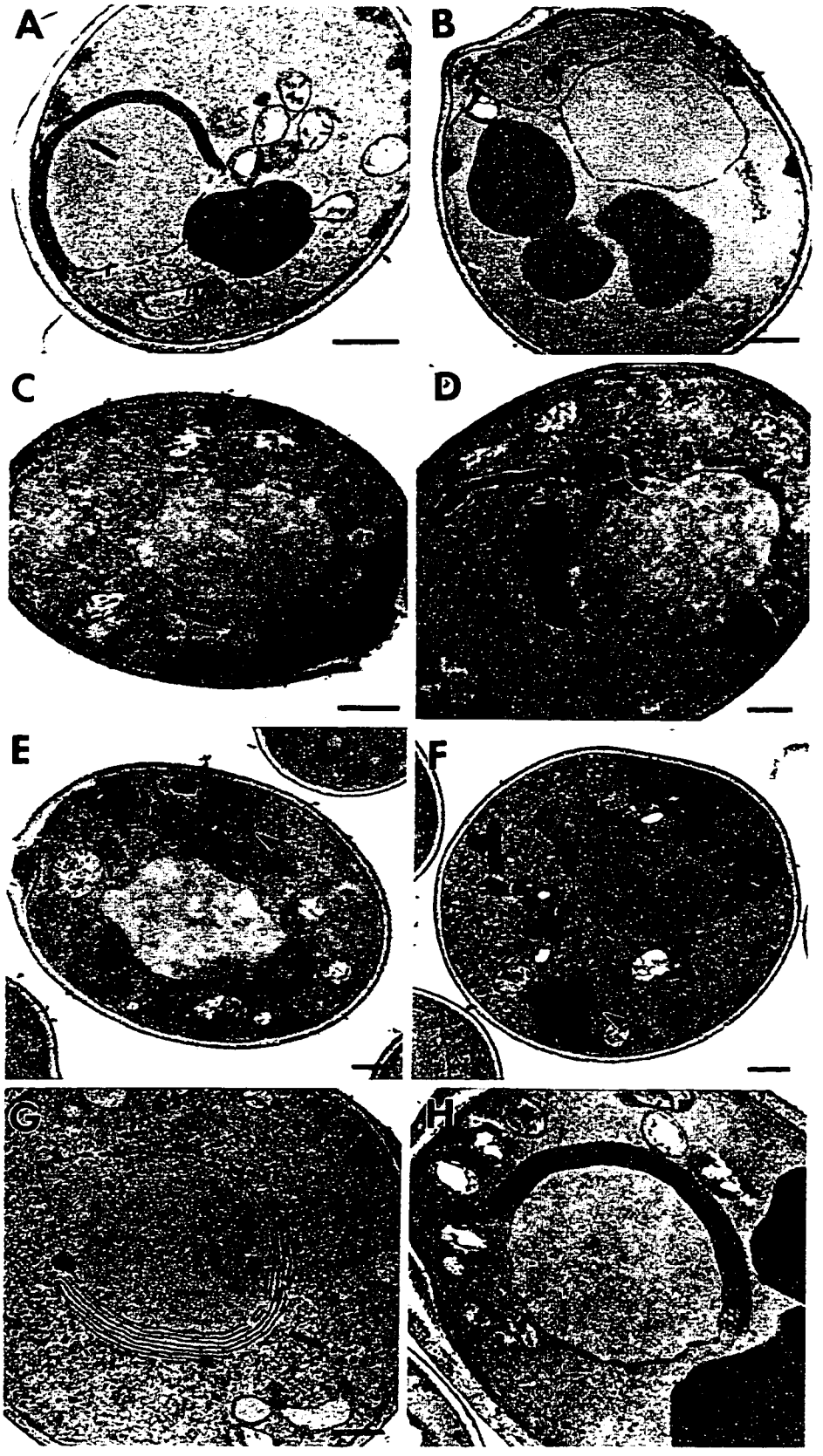
A
B
C
D
E
F
G
H

Figure 2.3 The abilities of different proteins to induce karmellae was unlikely to be due to quantitative differences in protein amount. The graph compares the relative levels of Hmg1p fusion proteins to the wild-type Hmg1p. The wild-type Hmg1p steady-state level was set to 1.0. For each strain, the percentage of cells in the population with karmellae was observed using $DiOC_6$. The expected percentage of karmellae reflected the percentage that would be present in cells expressing that amount of wild-type Hmg1p. This calculation assumes a linear relationship between amount of HMG-CoA reductase protein expressed and level of karmellae induced (Koning, unpublished results).

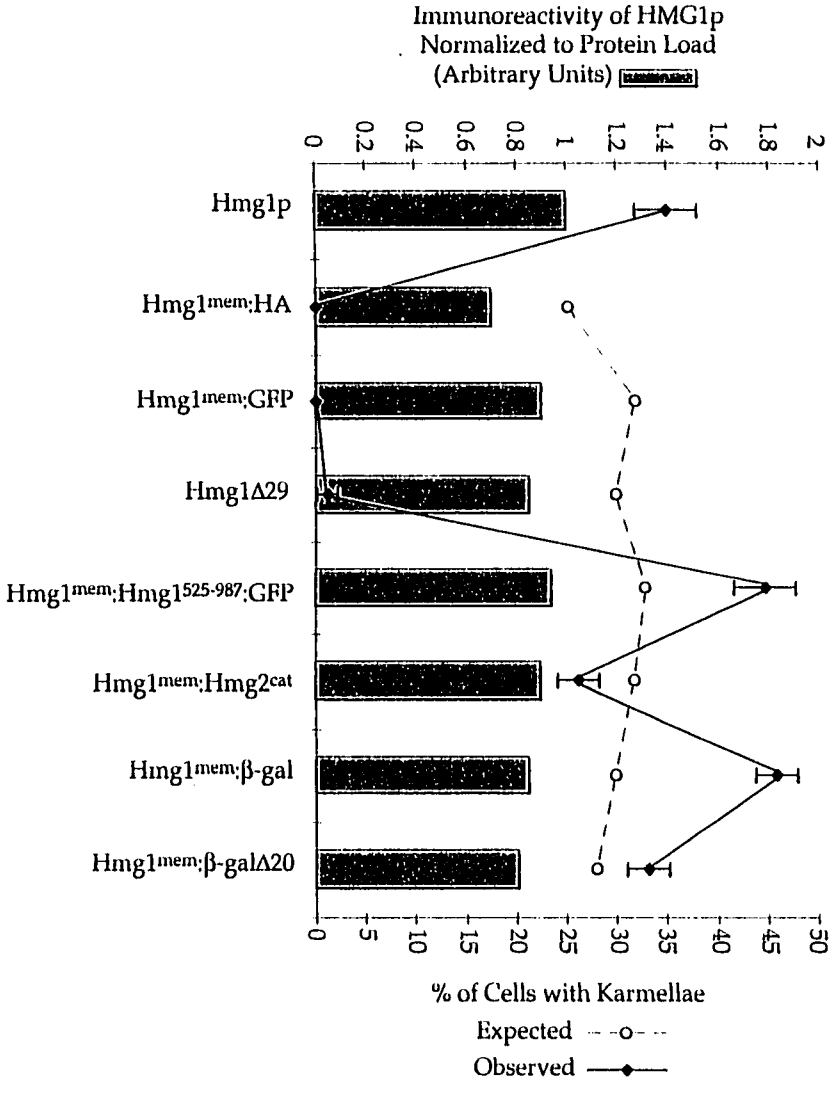
Immunoreactivity of HMG1p
Normalized to Protein Load
(Arbitrary Units)
0
0.2
0.4
0.6
0.8
1
1.2
1.4
1.6
1.8
2
Hmg1p
Hmg1mem:HA
Hmg1mem:GFP
Hmg1Δ29
Hmg1mem:Hmg1525-987:GFP
Hmg1mem:Hmg2cat
Hmg1mem:β-gal
Hmg1mem:β-galΔ20
0
5
10
15
20
25
30
35
40
45
50
% of Cells with Karmellae
Expected
Observed

Figure 2.4 The truncated Hmg1p variants had similar half-lives as the wild-type Hmg1p. Total cellular membranes were isolated and prepared for immunoblotting. At time zero, the culture was split into two flasks with one flask receiving 50 μg/ml cycloheximide (CHX). At subsequent times (2 and 4 hours), aliquots were removed for membrane isolation. (A) Intact Hmg1p (RWY 410) was detected using an antisera against the Hmg1p catalytic domain in the top panel. The lower panel is a duplicate gel stained with Coomassie. (B) The truncated $Hmg1^{mem}$:HA protein (RWY 614) was detected using the 12CA5 anti-HA antibody in the top panel. The lower panel is a duplicate gel stained with Coomassie. (C) The $Hmg1^{mem}$:GFP fusion (RWY 626) was detected using anti-GFP antisera in the top panel. The lower panel is a duplicate gel stained with Coomassie. (D) Hmg1Δ29p (RWY 406) was detected using an antisera against the Hmg1p catalytic domain in the top panel. The lower panel is a duplicate gel stained with Coomassie. (E) The graph compares the fusion protein levels, normalized to total protein loaded on the gel relative to the zero timepoint level for each protein. The relative levels of protein were determined for all timepoints and the percent decrease was calculated by comparing the 0 hour protein level to the 4 hour with cycloheximide protein level.

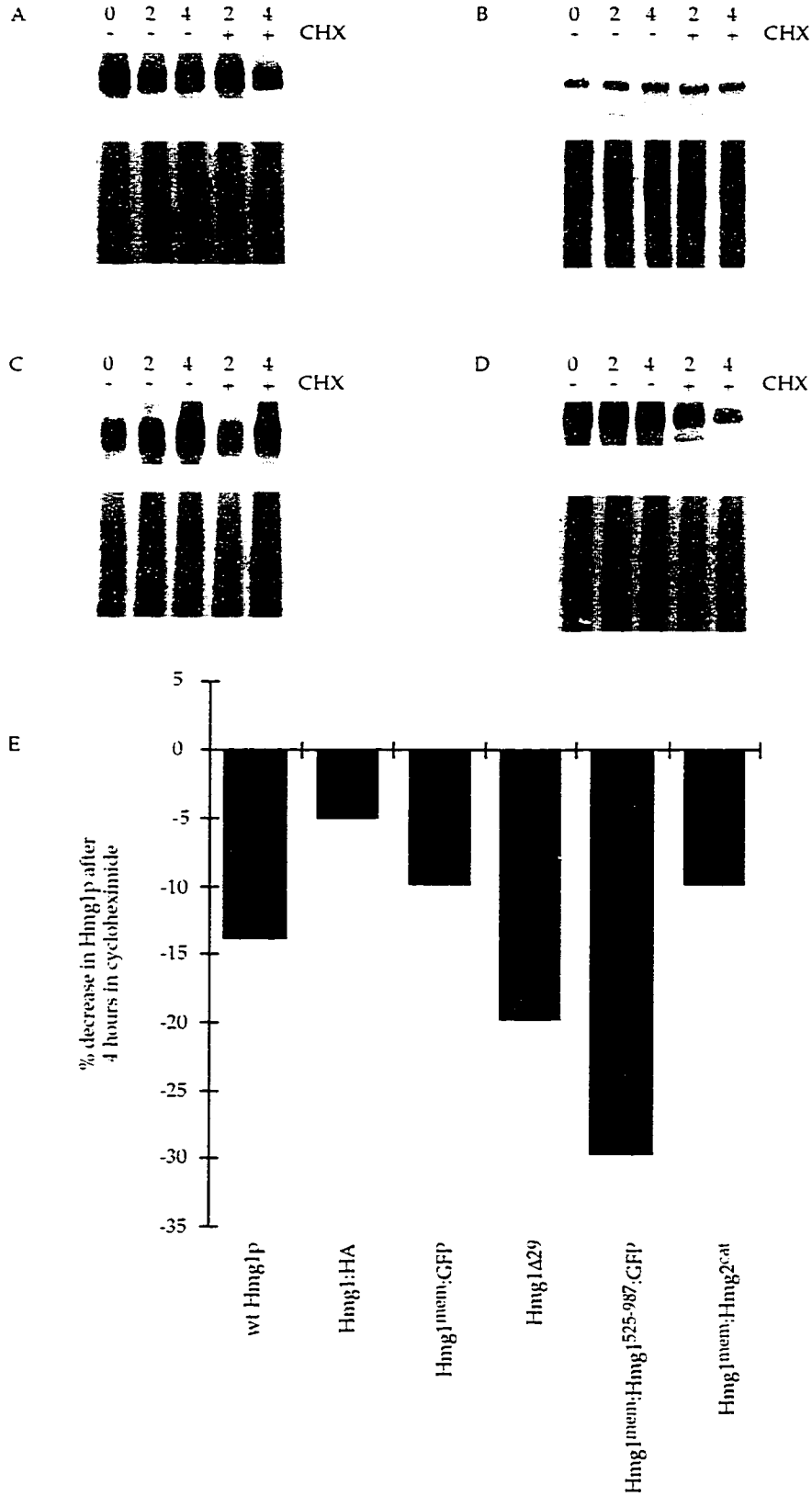
A
0 2 4 2 4
- - - + + CHX
B
0 2 4 2 4
- - - + + CHX
C
0 2 4 2 4
- - - + + CHX
D
0 2 4 2 4
- - - + + CHX
E
% decrease in Hmg1p after 4 hours in cycloheximide
5
0
-5
-10
-15
-20
-25
-30
-35
wt Hmg1p
Hmg1:HA
Hmg1mem:GFP
Hmg1Δ29
Hmg1mem:Hmg1525-987:GFP
Hmg1mem:Hmg2cat

Figure 2.5 Hmg1Δ29p was localized to the nuclear envelope in a pattern indistinguishable from the wild-type Hmg1p localization. Indirect immunofluorescent localization of Hmg1p or Kar2p is shown in panels A, C, E, and G. Localization of the nucleus in the same cells is shown by DAPI staining in panels B, D, F, and H. (A and B) Localization of elevated levels of wild-type Hmg1p was determined in cells of strain RWY 410 using an antibody to the catalytic domain of Hmg1p. (C and D) Localization of Kar2p in strain RWY 410 is shown for comparison. (E and F) Localization of elevated levels of Hmg1Δ29p in strain RWY 406 was determined by using an antibody to the catalytic domain of Hmg1p. (G and H) Localization of Kar2p in strain RWY 406 is shown for comparison. Bar, 5 μm.

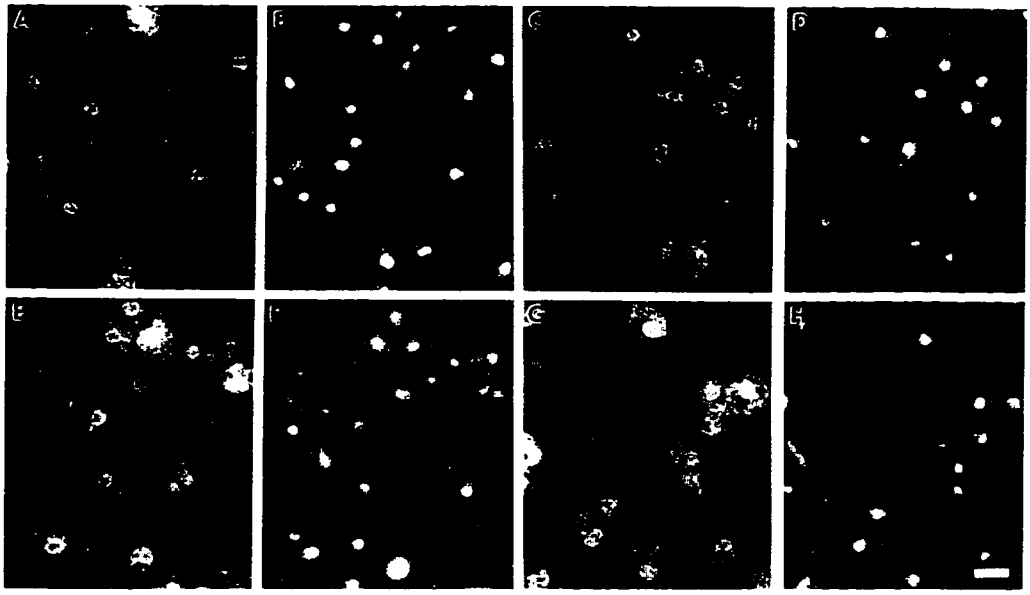
A
B
C
D
E
F
G
H

Figure 2.6 The truncated Hmg1^{mem}:HA protein was localized throughout the ER. Indirect immunofluorescent localization of the truncated Hmg1^{mem}:HA protein or Kar2p is shown in panels A and C. Localization of the nucleus in the same cells is shown by DAPI staining in panels B and D. (A and B) Localization of elevated levels of the truncated Hmg1^{mem}:HA protein in strain RWY 614 was detected by using 12CA5 anti-HA antibody. (C and D) Localization of Kar2p in strain RWY 614 is shown for comparison. Bar, 5 μm.

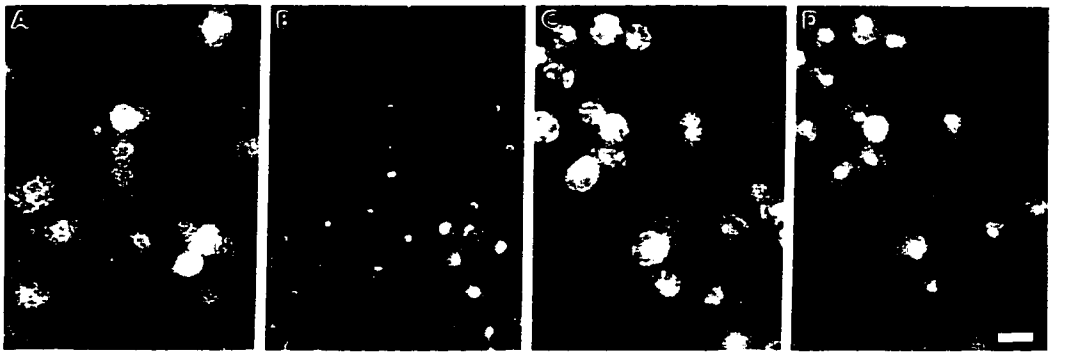
A
B
C
D

Figure 2.7 $Hmg1^{mem}$:GFP and $Hmg1^{mem}$:$Hmg1^{525-987}$:GFP were localized to the nuclear envelope with some peripheral ER staining. Indirect immunofluorescent localization of the GFP fusion proteins or Kar2p in shown in panels A, C, E, and G. Localization of the nucleus in the same cells is shown by DAPI staining in panels B, D, F, and H. (A and B) Localization of elevated levels of the $Hmg1^{mem}$:GFP protein in strain RWY 626 was determined by using a GFP antibody. (C and D) Localization of Kar2p in strain RWY 626 is shown for comparison. (E and F) Localization of elevated levels of the $Hmg1^{mem}$:$Hmg1^{525-987}$:GFP protein was determined in cells of strain RWY 621 using a GFP antibody. (G and H) Localization of Kar2p in strain RWY 621 is shown for comparison. Bar, 5 μm.

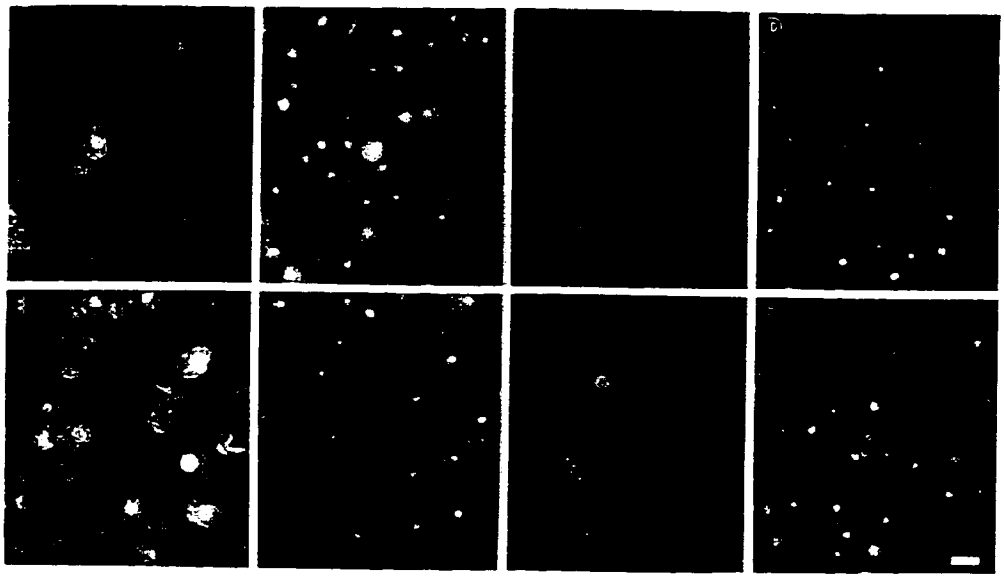
D

Table 2.2. Expression of the soluble Hmg1p catalytic domain interfered with the production of karmellae.

Strain	Protein expressed		% Karmellae[a]	Holoprotein[b]	Catalytic Domain[b]
	pGAL:Hmg1p	pGAPDH:Hmg1^{cat}			
RWY1494	X		41 ± 1	1.00	
RWY900		X	never seen		3.60
RWY1497	X	X	27 ± 1	1.05	3.30

[a] The % karmellae was determined from three independent experiments.

[b] After adjusting for total protein loaded, the amount of holoprotein or catalytic domain was normalized to holoprotein in RWY 1494.

Figure 2.8 $Hmg1^{mem}$:β-gal and $Hmg1^{mem}$:β-galΔ20 had similar half-lives compared to wild-type Hmg1p. Total cellular membranes were isolated and prepared for immunoblotting. At time zero, the culture was split into two flasks with one flask receiving 50 μg/ml cycloheximide (CHX). At subsequent times (2 and 4 hours), aliquots were removed for membrane isolation. (A) Hmg1:β-gal expressed in RWY 943 was detected using an antisera generated against the membrane domain of Hmg1p. (B) Hmg1:β-galΔ20 expressed in RWY 944 was detected using the same antisera as in (A).

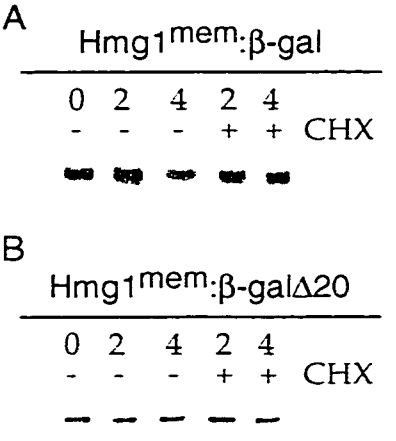
A
Hmg1mem:β-gal
0 2 4 2 4
- - - + + CHX
B
Hmg1mem:β-galΔ20
0 2 4 2 4
- - - + + CHX

Figure 2.9 $Hmg1^{mem}$:β-gal and $Hmg1^{mem}$:β-galΔ20 induced karmellae. Cells from both strains were fixed for electron microscopy. (A) RWY 943 cells expressing Hmg1:β-gal generate karmellae. (B) RWY 944 cells expressing Hmg1:β-galΔ20 also generate karmellae membranes. Bars, 0.5 μm.

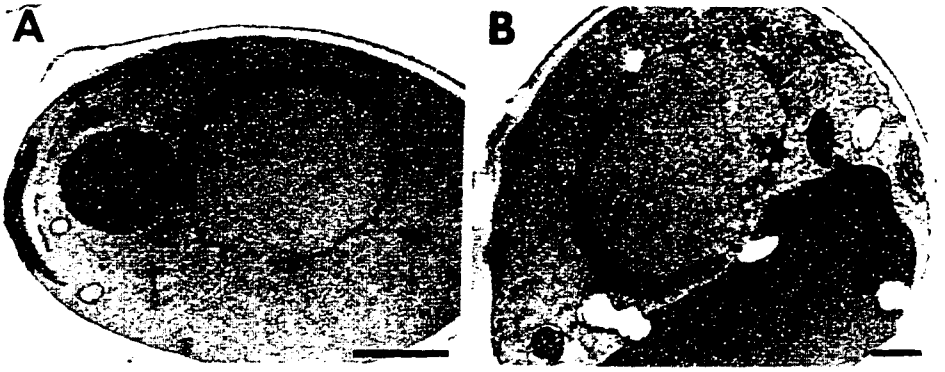
A
B

Figure 2.10 Hmg1^{mem}:β-gal and Hmg1^{mem}:β-galΔ20 were localized to the nuclear envelope. Indirect immunofluorescent localization of the Hmg1:β-galactosidase fusions or Kar2p is shown in panels A, C, E, and G. Localization of the nucleus in the same cells in shown by DAPI staining in panels B, D, F, and H. (A and B) Localization of elevated levels of the Hmg1:β-gal was determined in strain RWY 943 by using anti-β-gal antibody. (C and D) Localization of Kar2p in strain RWY 943 is shown for comparison. (E and F) Localization of elevated levels of the Hmg1:β-galΔ20 was determined in strain RWY 944 by using the same anti-β-gal antibody. (G and H) Localization of Kar2p in strain RWY 944 is shown for comparison. Bar, 5 μm.

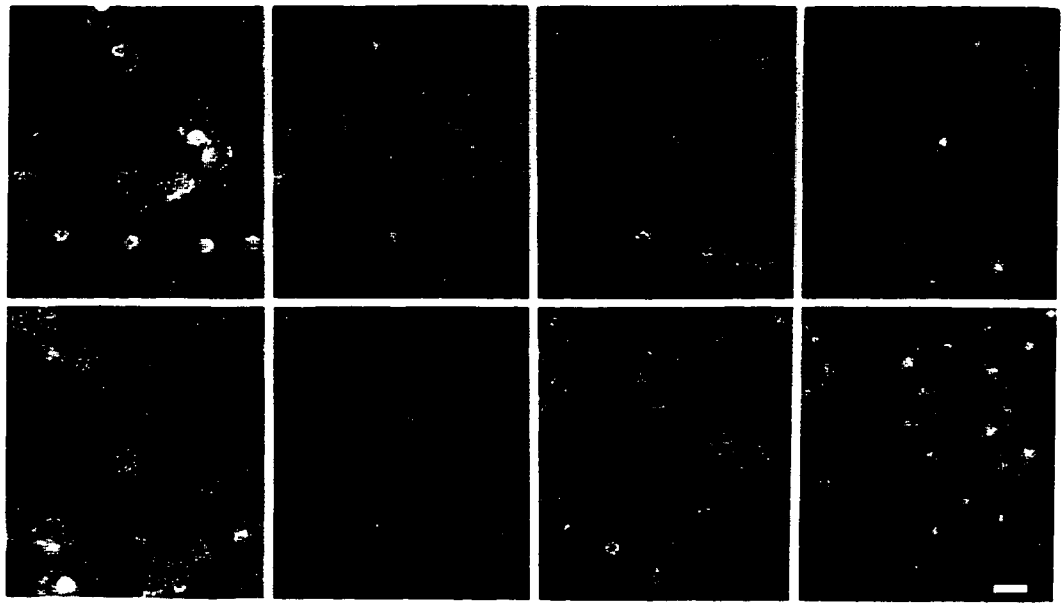

Table 2.3 Karmellae biogenesis from the Hmg1:β-galactosidase fusion proteins

Protein	% Karmellae[a]		β−gal activity[b]
	4 hr	8 hr	U/OD/min
Hmg1:β−galactosidase	46 ± 2	56 ± 2	236 ± 12
Hmg1:β−galΔ20	33 ± 2	37 ± 2	0.7 ± 0.4

[a] The % karmellae was determined from three independent experiments.

[b] β−galactosidase activity was determined from three independent experiments, running duplicate tubes for each experiment.

Chapter 3: Mutational analysis of the karmellae-inducing signal in HMG-CoA reductase of *Saccharomyces cerevisiae*

Abstract

In response to elevated levels of the integral membrane protein, HMG-CoA reductase, a variety of cell types, including yeast, assemble novel endoplasmic reticulum (ER) arrays. These membranes provide useful models to explore ER structure and function, as well as general features of membrane biogenesis and turnover. Yeast express two functional HMG-CoA reductase isozymes, Hmg1p and Hmg2p, that each induce morphologically different ER arrays. Hmg1p induces stacks of paired nuclear-associated membranes called karmellae. In contrast, Hmg2p induces peripheral ER membrane arrays and short nuclear-associated membrane stacks. In spite of the differences in cellular response to each isozyme, both Hmg1p and Hmg2p have similar structures, including a polytopic membrane domain containing eight predicted transmembrane helices. By examining a series of recombinant HMG-CoA reductase proteins, our laboratory previously demonstrated that the last ER-lumenal loop (Loop G) of the Hmg1p membrane domain contains a signal needed for proper karmellae assembly. Our goal was to determine the amino acids within Loop G that were critical for proper function of this signal. To this end, we have randomly mutagenized the Loop G sequence, expressed the mutagenized Hmg1p in yeast, and screened for inability to generate karmellae. Out of 4,000 strains with Loop G mutations, we isolated fifty-seven that were unable to efficiently assemble karmellae. We analyzed Loop G

sequences of mutant Hmg1p that were defective in their ability to induce karmellae as well as Hmg1p with Loop G mutations that did not affect their ability to induce karmellae assembly. Comparison of these mutations revealed that changes in charged amino acid residues led to a defect in karmellae biogenesis. Our hypothesis is that Loop G serves as a karmellae-inducing signal by mediating protein-protein interactions and that these charged amino acids may be important for maintaining the proper secondary structure of Loop G needed for these interactions.

Introduction

The mechanisms by which cells regulate the size, shape, and number of organelles remain a largely unanswered question in cell biology, in spite of widespread and dramatic examples of such regulation. For example, apparently in response to decreased ATP production, massive proliferation of mitochondria occurs in a variety of human myopathies (see Howell, 1999; Shoubridge, 1994 for review). The presence of these proliferated, frequently abnormal mitochondria results in the formation of "ragged red fibers," a diagnostic feature of the disease in skeletal muscle of affected individuals. Less dramatic alterations occur throughout a cell's lifespan, as it adjusts its structural features in response to environmental or physiological demands. The endoplasmic reticulum appears particularly amenable to such regulated alterations.

Regulation of ER morphology and amount is readily observed in response to treatments that elevate expression of ER proteins. For example, profound changes in ER structure accompany a variety of developmental changes, including B-cell differentiation (Shohat *et al.*, 1973; Zucker-Franklin *et al.*, 1988). In addition, proliferation of smooth ER occurs in response to exposure to phenobarbital, which induces expression of ER-resident cytochome P450s needed for drug detoxification

(Dallner *et al.*, 1966). ER proliferation can also be directly induced by experimental manipulation of a subset of ER-resident membrane proteins, including HMG-CoA reductase (Wright *et al.*, 1988), cytochrome b5 (Vergeres *et al.*, 1993), cytochrome P450s (Schunck *et al.*, 1991), the ribosome receptor (Wanker *et al.*, 1995), Sec12p (Nishikawa *et al.*, 1994), microsomal aldehyde dehydrogenase (Yamamoto *et al.*, 1996), and protease B negative 1 (Naik and Jones 1998). These experimental avenues for induction of ER proliferation offer interesting opportunities to discover how cells regulate ER structure and function in response to changes in protein level and should have general utility in understanding the regulation of organelle size and shape.

The yeast, *Saccharomyces cerevisae*, is a particularly useful organism for exploration of protein-induced ER proliferation. In addition to the standard advantages this organism provides from genetic and biochemical perspectives, it also affords a key benefit that revolves around the presence of functionally identical and structurally similar ER proteins that, nevertheless, induce morphologically different ER membrane arrays. These proteins, Hmg1p and Hmg2p, are both fully functional isozymes of a key enzyme in cholesterol synthesis, HMG-CoA reductase (Rine *et al.*, 1983; Basson *et al.*, 1986). This enzyme catalyzes the production of mevalonate, the first committed step in sterol biosynthesis and a major node for regulation of sterol biosynthesis (Goldstein and Brown, 1990). Although Hmg1p and Hmg2p both generate mevalonate, yeast cells respond differently to elevations in the amount of each protein. In response to Hmg1p, yeast assemble karmellae, an array of stacked ER membranes that are tightly associated with the nucleus (Wright *et al.*, 1988). In response to Hmg2p, yeast assemble short stacks of ER membranes that can be associated with the nucleus, plasma membrane, or be free in the cytoplasm (Koning *et al.*, 1996). A major goal of our laboratory is to understand the basis of yeast's different responses to these proteins.

Both Hmg1p and Hmg2p are large, structurally complex proteins that contain a cytoplasmically oriented catalytic domain and a polytopic membrane domain predicted to have eight transmembrane segments (Basson *et al.*, 1988; Lum *et al.*, 1996; Roitelman *et al.*, 1992). The membrane domain plays an essential role in two features of the protein: regulation of protein half-life (Gil *et al.*, 1985; Hampton and Rine, 1994; Jingami *et al.*, 1987) and induction of ER proliferation (Jingami *et al.*, 1987; Parrish *et al.*, 1995). In a series of systematic exchanges in which portions of the Hmg1p membrane domain were replaced with the corresponding region of Hmg2p, the final ER-lumenal loop between transmembrane segments 7 and 8 was found to be critical for karmellae assembly (Parrish *et al.*, 1995). Consequently, this region, referred to here as "Loop G," was presumed to contain key sequences necessary for mediating karmellae assembly. The experiments described in this paper extend this analysis to the amino acid level, revealing critical residues needed for efficient karmellae induction. Surprisingly, these residues include many that are conserved between Hmg1p and Hmg2p.

Materials and Methods

Strains and growth conditions

The yeast strains used in these studies are listed in Table 3.1. A description of the Loop G-encoded amino acid changes is found in Table 3.2. Strains were grown at 30°C on rich minimal medium (0.67% yeast nitrogen base without amino acids, 2% casamino acids, and 2% glucose or 2% galactose plus 3% sucrose or 2% galactose plus 3% raffinose) supplemented with the appropriate acids or nucleotide bases (Sherman *et al.*, 1986) or complete synthetic medium lacking histidine and uracil (CSM-his-ura) from Bio 101 (La Jolla, CA). Solid medium contained 2% agar (Sherman *et al.*, 1986).

Plasmids

The template used in the mutagenesis reactions and for the gapped plasmid was an allele of *HMG1* with introduced restriction sites flanking Loop G. *XhoI* and *SalI* sites were inserted at postitions corresponding to the amino terminal and carboxyl terminal ends of Loop G, respectively. The *XhoI* site at the amino terminus of Loop G was created by inserting 6 nucleotides (CTCGAG) after nucleotide 1272, inserting the amino acids Leu-Glu after residue number 424. The *SalI* site at the carboxyl terminus of Loop G was created by inserting 6 nucleotides (GTCGAC) after nucleotide 1494, inserting the amino acids Val-Asp after residue number 499 (Parrish *et al.*, 1995). Control experiments demonstrated that the HMG1 *XhoI -SalI* is fully functional with respect to providing lovastatin resistance and karmellae biogenesis when expressed at increased levels (Parrish *et al.*, 1995) .

The plasmid pCR452, a *CEN/ARS/URA3* vector containing *HMG1 XhoI -SalI* under the control of the *GAL1/10* promoter. To construct pCR452, the plasmid pAK85, containing a 690 bp *EcoRI-BamHI GAL1/10* promoter fragment in pRS306 (Sikorski and Hieter, 1989) was digested with *EcoRI*, blunt-ended, digested with *SalI*, and religated to create pCR448. This plasmid was cut with *SalI*, blunt-ended, digested with *KpnI*, and ligated to a 2.8 kb *SalI* (blunt-ended)-*Kpn*I fragment containing the first half of *HMG1* from pCR425. This plasmid, pCR450, was cut with *SphI* and *EcoRI* and ligated to the 1.5 kb *SphI -EcoRI* fragment containing the 5' end of *HMG1* with *XhoI*, *SalI* sites flanking Loop G from pMP320, creating pCR451. The plasmid, pCR452, was created by a 3-way ligation of a 2.4 kb *SpeI-SacI* fragment from pCR451(containing the *GAL1/10* promoter and the 5' end of *HMG1 XhoI -SalI*), a 1.8 kb *SacI-SalI* fragment from pDP152 (containing the 3' end of *HMG1*), and pRS316 (Sikorski and Hieter, 1989) digested with *SpeI* and *XhoI*. The vector containing the

GAL1/10 promoter without *HMG1*, pBM258, was previously described (Basson *et al.*, 1988).

To co-express wild-type Hmg1p with mutant Loop G Hmg1p proteins, a galactose-inducible *HMG1* plasmid, pAK266, was digested with *XhoI* and *SpeI* yielding a 4.3 kb fragment with the *GAL1/10* promoter and *HMG1*. This fragment was ligated into the *XhoI*, *SpeI* sites of pRS313 (Sikorski and Hieter, 1989) to produce pDP586, which consists of a *CEN-GAL1/10-HMG1* plasmid with the *HIS3* selectable marker.

Mutagenic PCR and co-transformation of yeast with a gapped plasmid and the mutagenized fragment

The plasmid, pCR452, was digested with *XhoI* and *SalI*, to produce a linearized, gapped vector lacking the 230 bp *XhoI-SalI* Loop G encoding sequences. The gapped plasmid was purified from agarose following electrophoresis using the Qiagen gel extraction kit (Qiagen, Valencia, CA). The Loop G encoding portion of *HMG1* was synthesized by PCR under mutagenic conditions (in the presence of Mn^{2+} and with skewed ratios of the dNTPs) as described (Muhlrad *et al.*, 1992; Cadwell and Joyce, 1992). Primers were designed for amplification of a 362 bp fragment including the region between the *XhoI* and *SalI* sites.

Yeast strain RWY720 (*hmg1::LYS2 ade his lys met pep4)* was co-transformed with 100 ng of the linearized gapped plasmid and 1 μg of the mutagenized fragment by lithium acetate transformation as described (Gietz *et al.*, 1992). The cells were plated on media containing yeast minimal salts, casamino acids, supplements, 2% galactose, 3% raffinose, and 150 μg/ml lovastatin. Lovastatin is a competitive inhibitor of HMG-CoA reductase (Alberts *et al.*, 1980). Consequently, expression of elevated levels of active Hmg1p is required for growth of yeast in the presence of lovastatin.

Colonies were picked from the transformation plate and patched onto a glucose plate, which served as a source plate to retrieve putative mutants. The patches were replica plated onto a galactose/raffinose plate, incubated for 16-20 hours at 30°C, and screened for the presence of karmellae by staining with $DiOC_6$ (Koning *et al.*, 1993). Strains with less than 63% of the wild-type karmellae level were retained for futher analysis to confirm the mutant phenotype.

DNA Sequencing

Plasmids from yeast were transformed into *E. coli* using a BRL protocol (BRL, Gaithersburg, MD) to allow subsequent purification of plasmid. Before sequence analysis, plasmids were digested with restriction enzymes to confirm the presence of the Loop G encoding region. Because the restriction sites *XhoI*, *SalI* which flank Loop G had compatible ends, it was possible that the gapped plasmid would religate onto itself without incorporating a Loop G encoding fragment. If restriction analysis demonstrated that the plasmid lacked the Loop G region, the plasmid was set aside. The Loop G deletion plasmids recovered from yeast produced a mutant karmellae phenotype. Restriction analysis showed that the remaining rescued plasmids did not have large deletions in *HMG1*, since *EcoRI*, *PstI*, *SalI*, and *SphI* digests of the plasmids gave the same banding pattern as the wild-type plasmid pCR452. Plasmid DNA was purified for sequencing using Invitrogen SNAP preps (Invitrogen, San Diego, CA). Sequencing was performed with the ABI PRISM dye terminator cycle sequencing ready reaction kit (Perkin Elmer, Foster City, CA) using primers that flank the Loop G region. These reactions were analyzed on an ABI 377 automated DNA sequencer (Perkin Elmer, Foster City, CA). Plasmid DNA was used to re-transform yeast to confirm that the karmellae assembly defect was plasmid-linked.

$DiOC_6$ staining

$DiOC_6$ (3,3'-dihexyloxacarbocyanine iodide) staining was performed as previously described (Koning *et al.*, 1993). Cells in log phase of growth were stained with 10μg/ml $DiOC_6$ (Kodak, Rochester, NY) per 10^7 cells using a 1mg/ml ethanolic stock. Stained cells were observed with conventional fluorescence optics, using a Nikon Microphot-FXA epifluorescence microscope with excitation (480+/-20nm) and barrier (535+/40nm) filters appropriate for fluorescein.

Immunofluorescence

Immunofluorescence was performed using a protocol similar to that described by Pringle (Pringle *et al.*, 1989). Log phase cells were fixed in 3.7% formaldehyde, treated with Zymolyase (United States Biological, Swampscott, MA) to partially remove their cell walls, and applied to multiwell slides (Koning *et al.*, 1996). Antisera generated against the carboxyl-terminal 15 amino acids of Hmg1p (LDII) was used at a 1:100 dilution. The incubation in primary antisera was for 1 hour at room temperature. The antibody solution was gently aspirated away and the cells were washed 5 times with TBST (25mM Trizma base, 3mM KCl, 140mM NaCl, 0.05% Tween-20). Then 10 μl of blocking solution (TBST+1% ovalbumin) was applied to each well. 10μl of secondary antibody (Goat anti-rabbit fluorescein conjugated, Cappel Organon Technika, Durham, NC) was diluted to 1:500 in blocking solution, centrifuged for 10 min, and applied to the appropriate wells. After 45 minutes, the secondary antibody was washed with TBST 5 times. 10μl of a 1:1000 dilution of 1mg/ml DAPI (Sigma, St. Louis, MO) in TBS was added to each well for 1 minute. After one rinse with TBS, a drop of Citifluor (Ted Pella, Redding, CA) was applied to each well, and the slide sealed with a coverslip and nailpolish. Each experiment included treatment of each strain with an antibody to detect tubulin (Yol1/34 (1:10 dilution) Accurate Chemical and

Scientific Company, Westbury, NY) as a positive control, and a treatment of secondary antibody only to detect any non-specific staining.

Protein preparation and immunoblotting

A membrane fraction was prepared for analysis of HMGR protein using immunoblots. Cells that had been growing in galactose medium for 8 hours were pelleted for 5 minutes at 834 X g in a clinical centrifuge. The cell pellets were stored at -80°C until processed. A total membrane fraction was prepared from the cells using modifications of methods previously described (Deschenes and Broach, 1987; Koning *et al.*, 1996). The pelleted membranes were resuspended in 25 µl lysis buffer/OD_{600} (0.3M sorbitol, 0.1M NaCl, 5mM MgCl2, and 20mM MOPS, pH 7.4) containing protease inhibitors (2 µg/ml each TPCK (N-tosyl-L-phenylalanine chloromethyl ketone), leupeptin, pepstatin A, aprotinin) found in complete tablets (Boehringer Mannheim Biochemica, Indianapolis, IN). The absorbance at 280 nm was measured for each sample in 1% SDS, and 100 A_{280} units were loaded on duplicate gels after heating at 65 ° C in 1X Laemmli sample buffer (0.03 M Tris-HCl, pH 6.8, 2% SDS, 10% glycerol, 5% β-mercaptoethanol, 0.005% Bromophenol blue) (Laemmli, 1970) for 10 min followed by a 5 min centrifugation at top speed in a microcentrifuge. Duplicate gels were run simultaneously; one gel was blotted to nitrocellulose and processed for immunodetection as described (Lum and Wright, 1995), and the duplicate gel was stained with Colloidal blue from Novex (San Diego, CA). The duplicate gel and the Western blot were digitized by scanning and analyzed using NIH Image 1.60 software as described (Lum and Wright, 1995).

Results

Identification of mutations in the Hmg1p Loop G sequence that prevent efficient induction of karmellae biogenesis.

Within the Hmg1p membrane domain, the final ER-lumenal loop that joins transmembrane segments seven and eight, Loop G, (see Figure 3.1) is critical for karmellae assembly (Parrish *et al.*, 1995). A reasonable hypothesis is that the corresponding region from other HMG-CoA reductases that induce karmellae also serves as the karmellae-inducing signal. Thus, one might be able to define the sequence requirements for karmellae induction by comparing the sequences of all HMG-CoA reductases that induce karmellae in *Saccharomyces cerevisiae*. Unfortunately, there is little sequence homology between the Loop G regions of *Saccharomyces cerevisiae* Hmg1p and human HMGR, making it difficult to predict which amino acids are critical for the function of this region. We set out to determine which residues within this 76 amino acid sequence were critical for the function of Loop G as a karmellae-inducing signal. To this end, we introduced random point mutations into the Loop G encoding portion of *HMG1* via mutagenic PCR (Muhlrad *et al.*, 1992; Cadwell and Joyce, 1992). Then yeast were transformed with the PCR product and a plasmid that was missing the Loop G region of *HMG1*. Resulting transformants usually contained an intact plasmid that had been reconstituted via recombination between the PCR product and the gapped plasmid, a process called gap repair (Rothstein, 1991). In addition, the haploid yeast used for this analysis lacked an intact chromosomal *HMG1* allele, so that the only Hmg1p produced by the cells would be expressed from the plasmid following gap repair. In our experiment, we did obtain transformants that contained a religated gapped plasmid missing the Loop G encoding region due to the compatibility of the restriction sites that flanked Loop G. To identify these Loop G deleted plasmids, we performed restriction digest analysis on all recovered plasmids.

Although we were interested in sequence determinants of the karmellae-inducing signal, any mutation in *HMG1* that resulted in low levels of the protein would also prevent karmellae assembly. To select for mutant Hmg1p proteins that continued to be expressed at high levels, the yeast transformants were grown in the presence of lovastatin, a competitive inhibitor of HMG-CoA reductase (Alberts *et al.*, 1980). Expression of high levels of active Hmg1p is necessary for growth on lovastatin plates. As shown in Figure 3.2, *hmg1*, *HMG2* cells containing the vector (RWY1086) were inviable on galactose, lovastatin solid medium. As expected, *hmg1*, *HMG2* cells harboring plasmids containing the *GAL1/10* promoter fused to either a wild-type *HMG1* or a Loop G mutant *HMG1* were viable on 150 μg/ml lovastatin medium. We then used fluorescence microscopy to examine the ability of the lovastatin-resistant colonies to assemble karmellae. Because karmellae remain in the mother cell at mitosis, karmellae are not observed in 100% of the cell population (Wright *et al.*, 1988). In populations of yeast that express wild-type Hmg1p from a galactose-inducible promoter (RWY864), approximately 40% of the population contain karmellae following 12 hours of induction on galactose medium. In our screen, we initially defined yeast as karmellae defective if they generated 25% karmellae or less.

Of 6,736 lovastatin-resistant colonies screened for their ability to generate karmellae, we examined the Loop G sequences from sixty randomly selected yeast strains that generated wild-type levels of karmellae. Twenty-two (37%) Loop G encoding sequences had the wild-type Loop G sequence. Therefore, approximately 63% of the Loop G encoding sequences contained mutations. After analysis of the Loop G sequences, we determined that 62% of the mutations were single nucleotide changes, 15% were two nucleotide changes, 11% were three nucleotide changes, and 12% were four or more nucleotide changes.

Using the wild-type calculations, we determined that 4.000 strains from our screen of 6,736 contained mutations. Fifty-seven strains with reduced levels of karmellae were retained for further analysis (Figure 3.3). The plasmids from the original mutants were passaged through *E. coli* and used to re-transform yeast to confirm that the mutant karmellae phenotype was plasmid-linked. We determined that seven of our karmellae-defective mutants did not exhibit plasmid-linked phenotypes. We then performed restriction digest analysis on the plasmids from the remaining fifty strains. Twenty-one plasmids were set aside because they were Loop G deletions in which the gapped plasmid had religated onto itself. Then, the mutated Loop G coding regions in the remaining twenty-nine plasmids that were unable to efficiently induce karmellae were sequenced. Twenty-six different Loop G sequences were obtained with three sequences isolated twice.

The positions of the predicted amino acid changes for the protein's with reduced ability to induce karmellae are shown in Figure 3.4 in relation to the wild-type Loop G sequences of Hmg1p and Hmg2p. The sequences for the Hmg1p and Hmg2p Loop G regions are 61% conserved with the majority of the amino acid differences clustered in the amino-terminal half of the loop (Basson *et al.*, 1988). Interestingly, the amino acid changes which reduced karmellae induction were located throughout the Loop G region and alter both conserved amino acids and non-conserved amino acids between Hmg1p and Hmg2p (Figure 3.4). This result was surprising because we had predicted that residues critical for karmellae assembly would be those residues that are not conserved between Hmg1p, which induces karmellae, and Hmg2p, which does not. Amino acid changes that do not affect the protein's ability to induce karmellae are shown in Figure 3.5. A comparison of the effects of single amino acids changes in Loop G is shown in Figure 3.6.

The inability to generate karmellae does not simply reflect lower amounts of Hmg1p.

Although lovastatin selection ensures that elevated levels of active Hmg1p are expressed, it is possible that the steady-state amount of mutant Hmg1p may not be equivalent to wild-type. If so, a trivial explanation for the reduction in karmellae is that the different mutant proteins are less abundant than the wild-type Hmg1p. We determined the relative protein levels of the 26 karmellae-defective mutants by immunoblots using antiserum directed against the catalytic domain of Hmg1p (Figure 3.7). Using the relative protein levels, we reclassified our 26 karmellae-defective mutants into two categories, mutations that produce less than 50% of expected karmellae levels and mutations that produce greater than 50% of expected karmellae levels. Karmellae assembly in the mutants was normalized to amounts of karmellae assembled in wild-type cells relative to the amount of Hmg1p expressed (Table 3.3). Of the eighteen mutants that produce less than 50% of expected karmellae levels, fifteen accumulated protein to significant levels (at least 70% of the wild-type protein level). This result indicated that the karmellae deficiency for these fifteen strains was not due to inadequate Hmg1p protein levels. The remaining three mutant proteins (I451N; L471S; and K460R, E461A) were present at reduced levels compared to the wild-type protein (less than 60% of the wild-type protein level). These results indicated that certain amino acid changes in Loop G can alter the accumulation of the protein. However, they also indicated that the phenotype of fifteen of the mutants with reduced karmellae was not explained by a decrease in the Hmg1p protein accumulation.

Mutations in Loop G that interfered with karmellae production did not cause mislocalization of the Hmg1p.

A mutation that altered the localization of Hmg1p might reduce the ability of the protein to signal for karmellae. To assess whether Loop G mutations influenced

the distribution of the Hmg1p, we localized three of the mutant Hmg1p proteins (D484H; N436K; K442M, L487P) with severely impaired karmellae signaling by indirect immunofluorescence. The mutant Hmg1p proteins were present in the nuclear envelope and the peripheral ER (Figure 3.8, C, D, E, F, G, H) producing a localization pattern that was indistinguishable from the localization pattern of the wild-type Hmg1p (Figure 3.8, A and B). The normal localization patterns of karmellae-defective Loop G mutant proteins demonstrated that the reduction in karmellae was not due to the mislocalization of the mutant Loop G proteins.

The mutant Loop G alleles are recessive to the wild-type HMG 1

HMGR functions as a dimer using contact sites in the catalytic domain (Edwards *et al.*, 1985; Basson *et al.*, 1987; Frimpong and Rodwell, 1994). If dimerization between Hmg1p molecules was important for karmellae assembly, the mutant Loop G Hmg1p proteins might exert a dominant negative effect by complexing with the wild-type protein and interfering with its ability to signal for karmellae assembly. Consequently, we examined karmellae assembly in three strains which simultaneously expressed the wild-type Hmg1p and one of three Loop G mutant Hmg1p proteins. These three Loop G mutant proteins were chosen because they were severely impaired for karmellae biogenesis, and their nuclear envelope localization was previously determined (Figure 3.8). As shown in Table 3.4, karmellae assembly was restored to 75% of the wild-type level in a strain expressing both the wild-type Hmg1p and a mutant Hmg1p. Therefore, the mutant Loop G alleles are recessive to the wild-type *HMG1*.

Discussion

As a step toward a more complete view of the sequence requirements needed for the function of a membrane-inducing signal, we carried out a mutational analysis of the Loop G coding region from *HMG1*. Based on our studies, we screened 4,000 strains with Loop G mutations and isolated only 29 karmellae-defective Loop G encoding sequences. This number indicates that less than 1% of the mutations in Loop G reduced that ability of the resulting protein to induce karmellae. The majority of amino acid changes were tolerated and did not compromise the karmellae-signaling function of this region. Finding tolerated changes is not surprising given that the HMG-CoA reductases from other species such as human and hamster can induce karmellae in *Saccharomyces cerevisiae* even though their Loop G sequences are different in amino acid composition and length (Figure 3.9; Wright *et al.*, 1990). The alignment of the Loop G amino acid sequences from different species was generated using the CLUSTAL X program (Thompson *et al.*, 1997). The fission yeast, *Schizosaccharomyces pombe*, generates karmellae in response to elevations in Hmg1p and Hmg2p from *Saccharomyces cerevisiae* and in response to the pombe *Hmg1*+ protein (Lum and Wright, 1995; Lum *et al.*, 1996).

We were able to isolate seven single amino acid changes in Loop G (N436K; D449V; S453T; V465A; V467D; D484H; and R498H) which dramatically reduced the ability of the protein to induce karmellae without affecting the protein's accumulation (Table 3.3). Of the remaining nine mutants that produce less than 50% of expected karmellae levels, three mutants (I451N; L471S; K460R, E461V) had a decreased protein level (Table 3.3). Therefore, the majority of the amino acid changes that we isolated did not alter the protein's accumulation but compromised the karmellae signal by another mechanism. One possible mechanism for preventing karmellae

assembly would be to cause mislocalization of the Hmg1p. We examined the localization of three of the mutant Hmg1p with severely impaired karmellae signaling. These three proteins localized to the nuclear envelope and the peripheral ER in a pattern similar to the wild-type Hmg1p (Figure 3.8). Therefore, these mutant proteins reduce karmellae signaling by a mechanism other than affecting protein steady-state levels or localization.

ER membrane arrays that appear similar to karmellae are induced by increasing the levels of certain ER membrane proteins, such as HMG-CoA reductase (Wright *et al.*, 1988), cytochrome P450 (Schunck *et al.*, 1991 542), cytochrome b5 (Vergeres *et al.*, 1993), the canine ribosomal receptor (Wanker *et al.*, 1995), and protease B negative 1 (Pbn1p) (Naik and Jones, 1998). These proteins capable of inducing karmellae do not share any sequence homology. Their shared feature is being anchored in the ER, and we postulate that they use a common pathway to signal for ER proliferation. Our working model for karmellae signaling is that proteins capable of inducing karmellae associate with specific lipids or proteins within the ER membrane. When the level of the karmellae-inducing protein increases, the associated proteins or lipids are concentrated in this region of the ER membrane. The altered ER composition affects the function of other proteins, ultimately leading to karmellae assembly.

This model is analogous to that imagined for the unfolded protein response. When "unfolded" proteins accumulate in the ER, the levels of free ER lumenal chaperones such as Kar2p decrease as the chaperones become complexed with the misfolded proteins. The decreased level of Kar2p is then believed to affect phosphorylation of the ER-resident kinase, Ire1p, which, in turn, activates Hac1p and ultimately upregulates expression of ER chaperones. In the case of karmellae, the

effects of Hmg1p on ER membrane composition is not yet clear. However, we do know, in our strains, that karmellae assembly does not directly involve the unfolded protein response pathway (Larson and Wright, 1998 YGM poster 240). Thus, identification of trans-acting factors needed for karmellae assembly should identify novel signaling pathways within the ER.

We propose that Loop G serves as a karmellae-inducing signal by mediating protein-protein interactions and that the critical residues maintain the contact sites required to permit these interactions. Because the mutant Loop G alleles were recessive to the wild-type *HMG1*, we conclude that the putative protein that interacts with Loop G is present in excess. Interestingly, none of the Loop G mutants that we identified was completely defective in karmellae assembly. Because the Loop G mutants generate 9-84% of expected karmellae levels, the mutant Loop G sequences are recognized as karmellae signals at some frequency. The Loop G deletion Hmg1p induced karmellae in 7% of the cell population, which seems to indicate that Loop G is not the only region recognized for karmellae signaling. We postulate that other regions of the Hmg1p membrane domain are recognized by the putative interacting protein.

The availability of karmellae-defective Hmg1p mutants will allow us to further explore the ER membrane biogenesis pathway through the identification of suppressors that restore wild-type karmellae levels. Suppressors may be mutant proteins that associate more efficiently with the mutated HMGR and restore karmellae, or they may bypass HMGR and signal for karmellae themselves. In either case, a more complete understanding of how HMG-CoA reductase leads to alterations in ER organization should follow identification of these genes. In turn, elucidation of the karmellae-signaling pathway will provide information concerning how a cell controls the size and shape of a key organelle, the endoplasmic reticulum.

Table 3.1 Yeast strains

Strain	Genotype
RWY 720	*MATa hmg1::LYS2 HMG2 ura3-52 his3Δ200 ade2-101 lys2-801 met TYR1 pep4 (parent strain for Loop G mutants)*
RWY 864	*MATa hmg1::LYS2 HMG2 ura3-52 his3Δ200 ade2-101 lys2-801 met TYR1 pep4 pCR452 (pGAL:Hmg1p; in pRS316 CEN6 URA3)*
RWY 1086	*MATa hmg1::LYS2 HMG2 ura3-52 his3Δ200 ade2-101 lys2-801 met TYR1 pep4 pBM150 (Ycp50 vector CEN4 URA3)*
RWY 1492	*MATa hmg1::LYS2 HMG2 ura3-52 his3Δ200 ade2-101 lys2-801 met TYR1 pep4 pDP586 (pGAl:Hmg1p in pRS313 CEN6 HIS3)*
RWY 1499	*MATa hmg1::LYS2 HMG2 ura3-52 his3Δ200 ade2-101 lys2-801 met TYR1 pep4 pDP586 (pGAL:Hmg1p) pCR463 (D484H)*
RWY 1501	*MATa hmg1::LYS2 HMG2 ura3-52 his3Δ200 ade2-101 lys2-801 met TYR1 pep4 pDP586 (pGAL:Hmg1p) pDP558 (K442M,L487P)*
RWY 1503	*MATa hmg1::LYS2 HMG2 ura3-52 his3Δ200 ade2-101 lys2-801 met TYR1 pep4 pDP586 (pGAL:Hmg1p) pDP638 (I451N)*

Table 3.2 Description of plasmids

Plasmid	Mutant Loop G Protein Expressed
pCR463	D484H Hmg1p
pCR465	V465A,I476F, L490P Hmg1p
pCR467	R498H Hmg1p
pDP555	D449V Hmg1p
pDP558	K442M,L487P Hmg1p
pDP560	K460R, E461A Hmg1p
pDP625	P469S Hmg1p
pDP629	V467D Hmg1p
pDP627	F426S, S466R, T468A Hmg1p
pDP630	E461V, L471S Hmg1p
pDP628	K474R Hmg1p
pDP638	I451N Hmg1p
pDP645	S453T Hmg1p
pDP654	N425D Hmg1p
pDP634	I419M, E424A,N436K Hmg1p
pDP635	A434V Hmg1p
pDP637	V465D, S466G Hmg1p
pDP641	Y439N, E457D, R491S Hmg1p
pDP643	Y439H, P448S, L489S Hmg1p
pDP646	N420I, V467A Hmg1p
pDP650	N436K Hmg1p
pDP651	F450C, I476F Hmg1p
pDP653	V465A Hmg1p
pDP655	F426L Hmg1p
pDP657	L471S Hmg1p
pDP677	V445G, P469L Hmg1p

Figure 3.1 The predicted topology for Hmg1p which highlights the localization of Loop G. Eight potential membrane spanning helices were identified in the hydropathy profiles of the membrane domains of Hmg1p, Hmg2p, and human HMGR. Previously, Hmg1p was identified as containing seven transmembrane-spanning helices. Further analysis predicted eight transmembrane helices by including the potential transmembrane span region 3. The asterisk indicates the controversial transmembrane span 3.

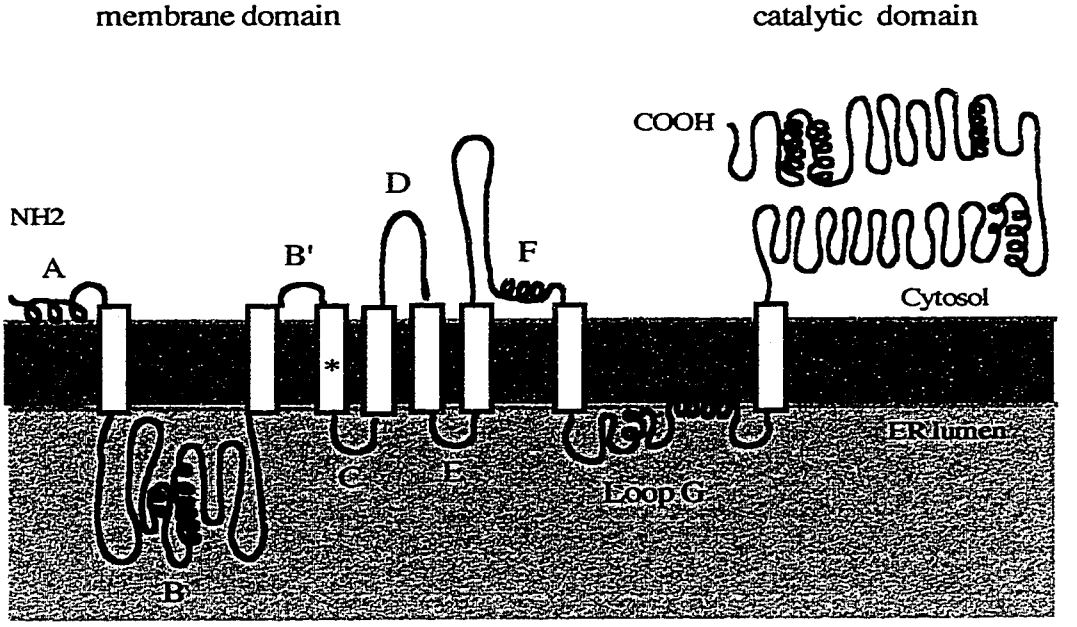
membrane domain
catalytic domain
COOH
NH2
A
B'
D
F
Cytosol
*
ER lumen
C
E
Loop G
B

Figure 3.2 Elevated levels of the wild-type Hmg1p or elevated levels of the mutant Loop G proteins conferred lovastatin resistance to the cells expressing these proteins. Single colonies were streaked from a glucose plate onto a galactose, sucrose plate or onto a galactose, sucrose plus lovastatin plate.

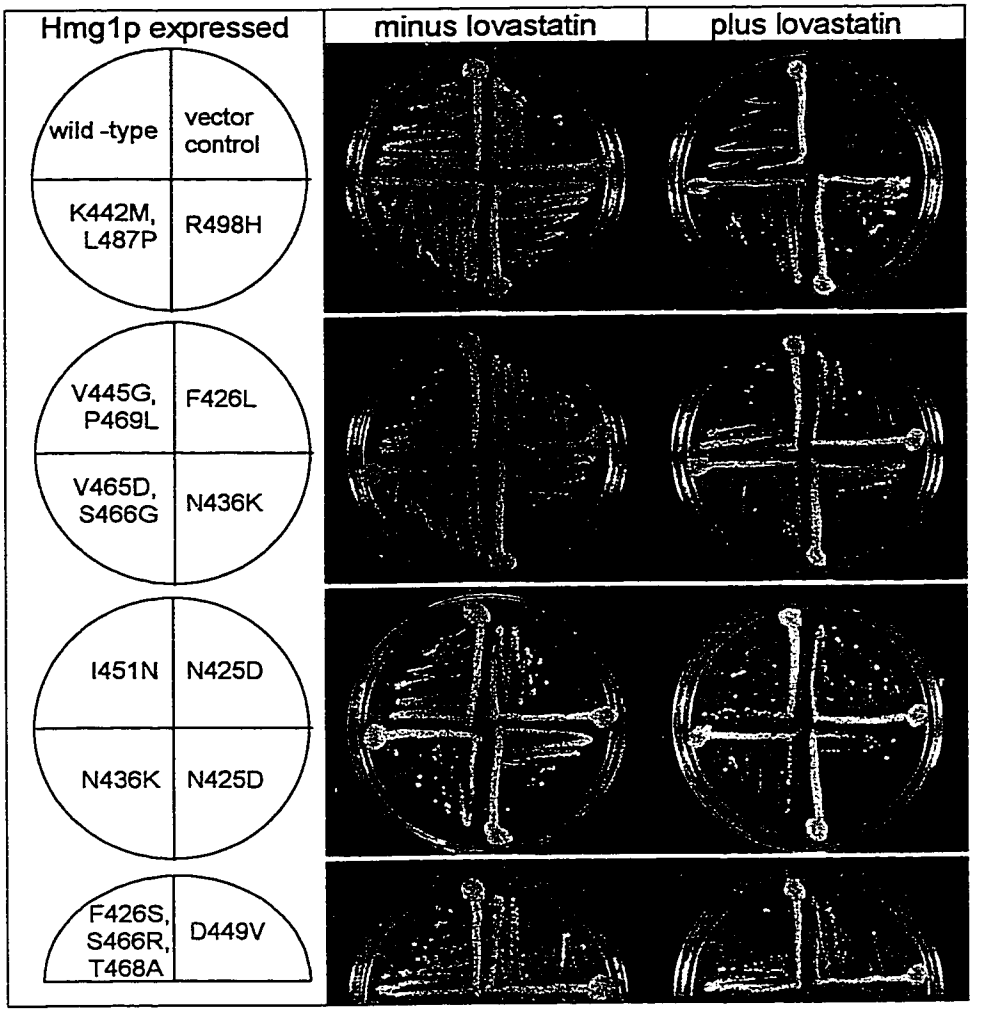
Hmg1p expressed
minus lovastatin
plus lovastatin
wild -type
vector control
K442M, L487P
R498H
V445G, P469L
F426L
V465D, S466G
N436K
I451N
N425D
N436K
N425D
F426S, S466R, T468A
D449V

6,736 lovastatin-resistant colonies screened

4,000 colonies with mutations in Loop G

3,943 colonies generated wild-type karmellae levels

57 colonies with reduced karmellae levels

21 Loop G deletion plasmids

7 mutants with non-plasmid linked phenotypes

29 mutants with plasmid-linked phenotypes

Figure 3.3 A flowchart showing the breakdown of yeast isolated in our screen based on phenotype.

Figure 3.4 Summary of Loop G mutations that reduced the ability of the protein to induce karmellae. The positions of the amino acid changes are shown below the wild-type Loop G sequences for Hmg1p and Hmg2p.

Protein	Sequence	Normalized Karmellae*
Hmg2p	VFTDKLNATILNTVYFDSTIYSLPNFINYKDIGNLSNQVIISVLPKQYYTPLKKYHQIEDSVLLIIDSVSNAIRDQ	none**
Hmg1p	NFGANWVNDAFNSLYFDKERVSLPDFITSNASENFKEQAIVSVTPLLYYKPIKSYQRIEDMVLLLLRNVSVAIRDR	1.00
Mutations that produce less than 50% of expected karmellae levels		
N436K	NFGANWVNDAF**K**SLYFDKERVSLPDFITSNASENFKEQAIVSVTPLLYYKPIKSYQRIEDMVLLLLRNVSVAIRDR	.23
D449V	NFGANWVNDAFNSLYFDKERVSLP**V**FITSNASENFKEQAIVSVTPLLYYKPIKSYQRIEDMVLLLLRNVSVAIRDR	.35
I451N	NFGANWVNDAFNSLYFDKERVSLPDF**N**TSNASENFKEQAIVSVTPLLYYKPIKSYQRIEDMVLLLLRNVSVAIRDR	.38
S453T	NFGANWVNDAFNSLYFDKERVSLPDFITT**T**NASENFKEQAIVSVTPLLYYKPIKSYQRIEDMVLLLLRNVSVAIRDR	.35
V465A	NFGANWVNDAFNSLYFDKERVSLPDFITSNASENFKEQAI**A**SVTPLLYYKPIKSYQRIEDMVLLLLRNVSVAIRDR	.25
V467D	NFGANWVNDAFNSLYFDKERVSLPDFITSNASENFKEQAIVS**D**TPLLYYKPIKSYQRIEDMVLLLLRNVSVAIRDR	.36
L471S	NFGANWVNDAFNSLYFDKERVSLPDFITSNASENFKEQAIVSVTPLI**S**YYKPIKSYQRIEDMVLLLLRNVSVAIRDR	.46
D484H	NFGANWVNDAFNSLYFDKERVSLPDFITSNASENFKEQAIVSVTPLLYYKPIKSYQRIE**H**MVLLLLRNVSVAIRDR	.21
R498H	NFGANWVNDAFNSLYFDKERVSLPDFITSNASENFKEQAIVSVTPLLYYKPIKSYQRIEDMVLLLLRNVSVAI**H**DR	.15
K442M,L487P	NFGANWVNDAFNSLYFD**M**ERVSLPDFITSNASENFKEQAIVSVTPLLYYKPIKSYQRIEDMV**P**LLLRNVSVAIRDR	.09
V445G,P469L	NFGANWVNDAFNSLYFDKER**G**SLPDFITSNASENFKEQAIVSVT**L**LLYYKPIKSYQRIEDMVLLLLRNVSVAIRDR	.34
K460R,E461A	NFGANWVNDAFNSLYFDKERVSLPDFITSNASENF**RA**QAIVSVTPLLYYKPIKSYQRIEDMVLLLLRNVSVAIRDR	.36
F426S,S466R,T468A	NI**S**GANWVNDAFNSLYFDKERVSLPDFITSNASENFKEQAIV**R**V**A**PLLYYKPIKSYQRIEDMVLLLLRNVSVAIRDR	.25
Y439H,P448S,L489S	NFGANWVNDAFNSL**H**FDKERVSL**S**DFITSNASENFKEQAIVSVTPLLYYKPIKSYQRIEDMVLL**S**LRNVSVAISDR	.38
Y439N,E457D,R491S	NFGANWVNDAFNSL**N**FDKERVSLPDFITSNAS**D**NFKEQAIVSVTPLLYYKPIKSYQRIEDMVLLLL**S**NVSVAIRDR	.43
V465A,I476F,L490P	NFGANWVNDAFNSLYFDKERVSLPDFITSNASENFKEQAI**A**SVTPLLYYKP**F**KSYQRIEDMVLLL**P**RNVSVAIRDR	.42
Mutations that change an amino acid in Loop G and in the preceeding transmembrane domain		
N420I, V467A	NFGANWVNDAFNSLYFDKERVSLPDFITSNASENFKEQAIVS**A**TPLLYYKPIKSYQRIEDMVLLLLRNVSVAIRDR	.46
I419M,E424A,N436K	NFGANWVNDAF**K**SLYFDKERVSLPDFITSNASENFKEQAIVSVTPLLYYKPIKSYQRIEDMVLLLLRNVSVAIRDR	.15
Mutations that produce greater than 50% of expected karmellae levels		
N425D	D**F**GANWVNDAFNSLYFDKERVSLPDFITSNASENFKEQAIVSVTPLLYYKPIKSYQRIEDMVLLLLRNVSVAIRDR	.71
F426L	NI**L**GANWVNDAFNSLYFDKERVSLPDFITSNASENFKEQAIVSVTPLLYYKPIKSYQRIEDMVLLLLRNVSVAIRDR	.53
A434V	NFGANWVND**V**FNSLYFDKERVSLPDFITSNASENFKEQAIVSVTPLLYYKPIKSYQRIEDMVLLLLRNVSVAIRDR	.63
P469S	NFGANWVNDAFNSLYFDKERVSLPDFITSNASENFKEQAIVSVT**S**LLYYKPIKSYQRIEDMVLLLLRNVSVAIRDR	.84
K474R	NFGANWVNDAFNSLYFDKERVSLPDFITSNASENFKEQAIVSVTPLLYY**R**PIKSYQRIEDMVLLLLRNVSVAIRDR	.80
F450C,I476F	NFGANWVNDAFNSLYFDKERVSLPD**C**ITSNASENFKEQAIVSVTPLLYYKP**F**KSYQRIEDMVLLLLRNVSVAIRDR	.53
E461V,L471S	NFGANWVNDAFNSLYFDKERVSLPDFITSNASENF**V**QAIVSVTPLI**S**YYKPIKSYQRIEDMVLLLLRNVSVAIRDR	.76
V465D,S466G	NFGANWVNDAFNSLYFDKERVSLPDFITSNASENFKEQAI**DG**VTPLLYYKPIKSYQRIEDMVLLLLRNVSVAIRDR	.60

***Karmellae assembly was normalized to amounts of karmellae assembled in wild-type cells relative to the amount of Hmg1p expressed.**

****Hmg2p does not induce karmellae but instead induces morphologically distinct membranes in 40% of cells.**

Figure 3.5 Summary of Loop G mutations that did not impair the ability of the protein to signal for karmellae. The positions of the amino acid changes are shown below the wild-type Loop G sequences for Hmg1p and Hmg2p.

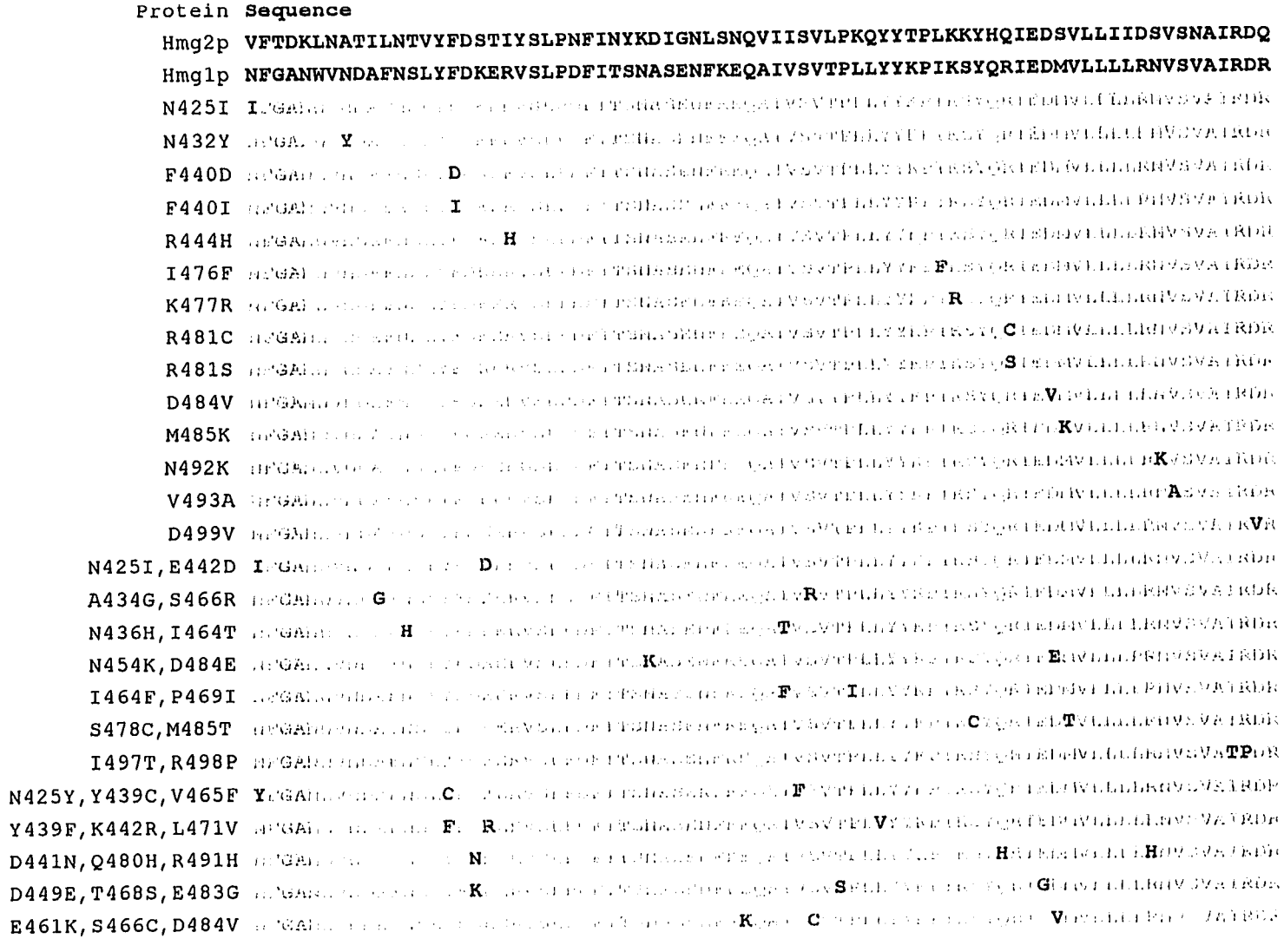
Protein Sequence
Hmg2p VFTDKLNATILNTVYFDSTIYSLPNFINYKDIGNLSNQVIISVLPKQYYTPLKKYHQIEDSVLLIIDSVSNAIRDQ
Hmg1p NFGANWVNDAFNSLYFDKERVSLPDFITSNASENFKEQAIVSVTPLLYYKPIKSYQRIEDMVLLLLRNVSVAIRDR
N425I
N432Y
F440D
F440I
R444H
I476F
K477R
R481C
R481S
D484V
M485K
N492K
V493A
D499V
N425I,E442D
A434G,S466R
N436H,I464T
N454K,D484E
I464F,P469I
S478C,M485T
I497T,R498P
N425Y,Y439C,V465F
Y439F,K442R,L471V
D441N,Q480H,R491H
D449E,T468S,E483G
E461K,S466C,D484V

Figure 3.6 Comparison of the single amino acid changes in Loop G that have no effect on karmellae synthesis (top lines, in green) with those that decrease or prevent karmellae synthesis (lower line, in red). Residues that are conserved in all known yeast Loop G sequences are shown in blue.

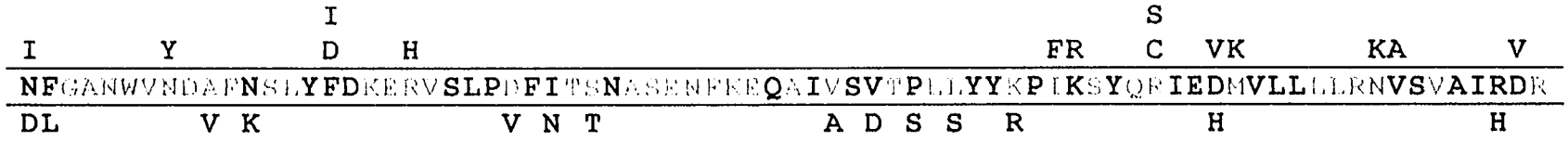
I
Y
I
D
H
S
C
FR
VK
KA
V
NFGANWVNDAFNSLYFDKERVSLPDFITSNASENFKEQAIVSVTPLLYYKPIKSYQFIEDMVLLLLRNVSVAIRDR
DL
V K
V N T
A D S S R
H
H

Figure 3.7 Comparison of the Hmg1p levels for wild-type Hmg1p versus the mutant Hmg1p proteins. Total cellular membranes were isolated and prepared for immunoblotting. Wild-type Hmg1p and the mutant Loop G proteins were detected using an antisera against the Hmg1p catalytic domain. The expression level of the protein was normalized for total protein loaded and compared to the value of 1.0 given to wild-type Hmg1p levels.


0.5 K474R
0.8 S453T
1.0 A434V
1.0 I419M,E424A,N436K
0.7 N420I,V467A
1.0 F450C,I476F
1.0 V465A
0.3 V465D,S466G

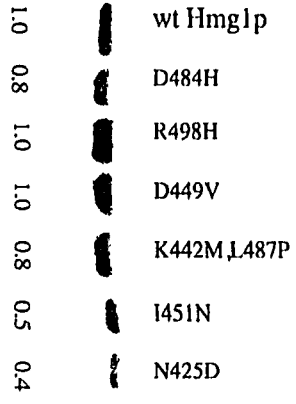
1.0 wt Hmg1p
0.8 D484H
1.0 R498H
1.0 D449V
0.8 K442M,L487P
0.5 I451N
0.4 N425D


0.8 F426S,S466R,T468A
0.9 Y439H,P448S,L489S
1.0 F426L
1.0 Y439N,E457D,R491S
0.6 E461V,L471S
0.6 K460R,E461A
0.5 P469S

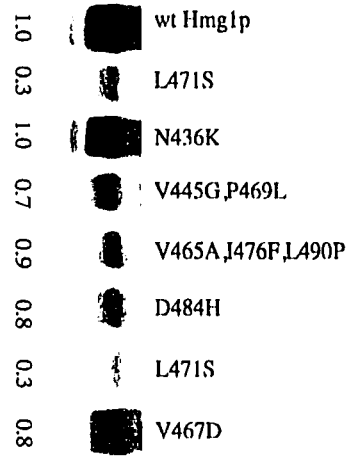
1.0 wt Hmg1p
0.3 L471S
1.0 N436K
0.7 V445G,P469L
0.9 V465A,I476F,L490P
0.8 D484H
0.3 L471S
0.8 V467D

Table 3.3 The inability to generate karmellae did not correlate with the level of Hmg1p expressed.

Hmg1p variant	Hmg1p levels[a]	observed % karmellae	expected % karmellae[b]	Normalized karmellae
wild-type Hmg1p	1.0	40	40	1.00
N425D Hmg1p	0.4	10	14	.71
F426L Hmg1p	1.0	21	40	.53
A434V Hmg1p	1.0	25	40	.63
N436K Hmg1p	1.0	9	40	.23
D449V Hmg1p	1.0	14	40	.35
I451N Hmg1p	0.5	8	21	.38
S453T Hmg1p	0.8	12	34	.35
V465A Hmg1p	1.0	10	40	.25
V467D Hmg1p	0.8	12	33	.36
P469S Hmg1p	0.5	16	19	.84
L471S Hmg1p	0.3	6	13	.46
K474R Hmg1p	0.5	16	20	.80
D484H Hmg1p	0.8	7	33	.21
R498H Hmg1p	1.0	6	40	.15
N420I, V467A Hmg1p	0.7	13	28	.46
K442M, L487P Hmg1p	0.8	3	32	.09
V445G, P469L Hmg1p	0.7	10	29	.34
F450C, I476F Hmg1p	1.0	21	40	.53
K460R, E461A Hmg1p	0.6	8	22	.53
E461A, L471S Hmg1p	0.6	19	25	.76
V465D, S466G Hmg1p	0.3	8	13	.60
I419M, E424A, N436K Hmg1p	1.0	6	40	.15
F426S, S466R, T468A Hmg1p	0.8	8	32	.25
Y439N, E457D, R491S Hmg1p	1.0	15	40	.38
Y439H, P448S, L489S Hmg1p	0.9	23	34	.43
V465A, I476F, L490P Hmg1p	0.9	15	36	.42

[a] After adjusting for total protein loaded, the amount of mutant Hmg1p was normalized to wild-type Hmg1p.
[b] Expected % karmellae given the level of Hmg1p within the cell.

Figure 3.8 The mutant Loop G proteins localized to the nuclear envelope. Localization of elevated levels of wild-type Hmg1p and three of the mutant Loop G proteins by indirect immunofluorescence Indirect immunofluorescent localization of Hmg1p is shown in panels A, C, E, and G. Localization of the nucleus in the same cells is shown by DAPI staining in panels B, D, F, and H. (A and B) Localization of elevated levels of wild-type Hmg1p was determined in cells of strain RWY 864 using an antibody to the catalytic domain of Hmg1p. (C and D) Localization of elevated levels of I451N Hmg1p in strain RWY 1088 was determined by using the same antibody. (E and F) Localization of elevated levels of D484H in RWY 889 was determined using the same antibody. (G and H) Localization of elevated levels of K442M, L487P Hmg1p in RWY 927 was determined using the same antibody. Bar, 5 μm.

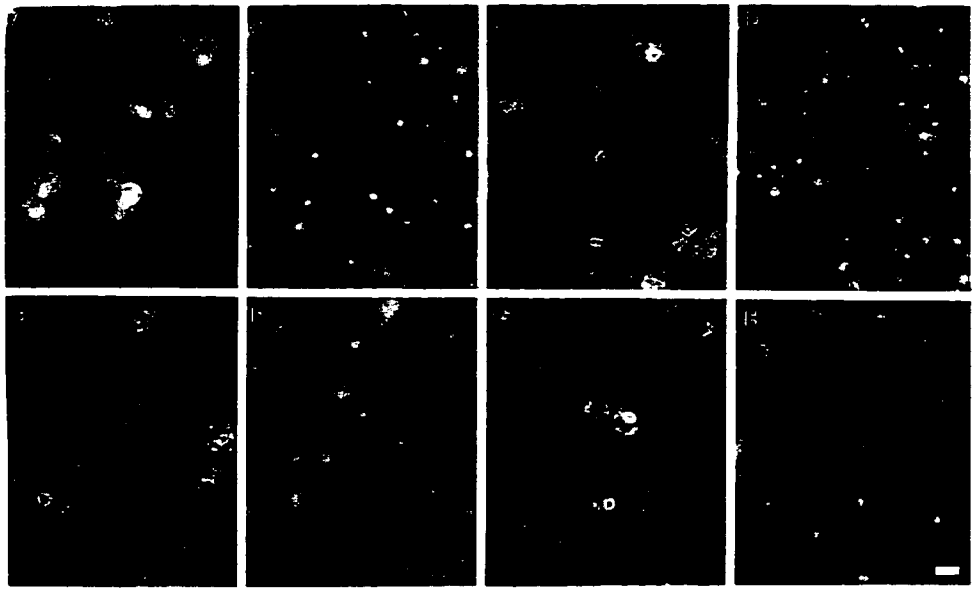

Table 3.4 Karmellae assembly in cells co-expressing wild-type Hmg1p together with mutant Hmg1p

Protein(s)	**% karmellae**
wild-type Hmg1p alone	41%
Hmg1(D484H)p alone	7%
wild-type Hmg1p + Hmg1(D484H)p	30%
Hmg1(K442M, L487P)p alone	3%
wild-type Hmg1p + Hmg1(K442M, L487P)p	32%
Hmg1(I451N) p alone	10%
wild-type Hmg1p + Hmg1(K442M, L487P)p	30%

Figure 3.9 Alignment of Loop G amino acid sequences for HMG-CoA reductase of *Saccharomyces cerevisiae*, *Schizosaccharomyces pombe*, human, and Syrian hamster. These HMG-CoA reductase proteins generated karmellae when expressed at elevated levels in *Saccharomyces cerevisiae* except for pombe reductase which has not been tested. In *Schizosaccharomyces pombe*, elevated levels of Hmg1p and Hmg2p from *Saccharomyces cerevisiae* induce karmellae as well as the pombe Hmg1+ protein (Lum and Wright, 1995; Lum *et al.*, 1996). This alignment was generated using the CLUSTAL X program (Thompson *et al.*, 1997).

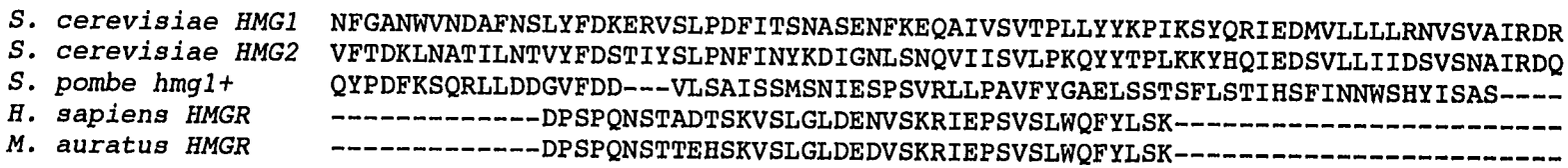
S. cerevisiae HMG1 NFGANWVNDAFNSLYFDKERVSLPDFITSNASENFKEQAIVSVTPLLYYKPIKSYQRIEDMVLLLLRNVSVAIRDR
S. cerevisiae HMG2 VFTDKLNATILNTVYFDSTIYSLPNFINYKDIGNLSNQVIISVLPKQYYTPLKKYHQIEDSVLLIIDSVSNAIRDQ
S. pombe hmg1+ QYPDFKSQRLLDDGVFDD---VLSAISSMSNIESPSVRLLPAVFYGAELSSTSFLSTIHSFINNWSHYISAS----
H. sapiens HMGR ----------DPSPQNSTADTSKVSLGLDENVSKRIEPSVSLWQFYLSK----------
M. auratus HMGR ----------DPSPQNSTTEHSKVSLGLDEDVSKRIEPSVSLWQFYLSK----------

Chapter 4: Future Directions

The karmellae-signaling pathway

I started graduate school with an interest in exploring a signaling pathway in detail. Even though membranes are essential structures for many cellular functions, surprisingly little is known about how cells regulate the assembly and degradation of specific membranes. The long term objective guiding my work in the Wright lab was to dissect the karmellae signaling pathway. Karmellae, nuclear-associated membranes, are built in yeast in response to mammalian HMGR or yeast HMGR. The cellular response of building ER arrays is conserved between mammalian cells and yeast when the levels of HMG-CoA reductase are increased. Mammalian cells do not build karmellae, but rather an expansion of ER tubules called crystalloid ER (Wright *et al.*, 1990). Crystalloid ER are known to house HMGR and at least 9 other proteins (Kochevar and Anderson, 1987). Unfortunately, the identities of the 9 other proteins remain unknown, but we suspect these proteins to be smooth ER components and not unique to crystalloid ER.

Unlike mammalian cells or *S. pombe*, *Saccharomyces cerevisiae* contains two genes for HMGR which both encode functional proteins. Increased levels of Hmg1p induce nuclear-associated stacks of ER, called karmellae, with some peripheral membrane arrays. Elevated levels of Hmg2p, on the other hand, lead to peripheral ER stacks with some shorter karmellae on the nucleus. Koning *et al.* demonstrated that Hmg1p and Hmg2p are localized to different ER subcompartments at elevated levels and that the protein composition of these subcompartments can be regulated (Koning *et al.*, 1996). Specifically, Kar2p, the ER-lumenal chaperone, was excluded from the Hmg2-

type membrane proliferations but not from the Hmg1-induced proliferations. A membrane-spanning ER protein, Sec61p, was localized to both types of ER arrays (Koning *et al.*, 1996). The ability to control membrane synthesis by altering the amount of HMGR provides an opportunity to analyze the regulation of membrane assembly and composition.

How do cells regulate the assembly of specific membranes?

We would like to develop a molecular description of: how a cell determines the need for additional membranes, how the components of the new membrane are assembled, and what determines the localization and turnover of the resulting membranes. My thesis work increased our understanding of the first part of the description, how a cell determines the need for additional membranes. When my 2 hybrid screen to identify proteins that interacted with the Loop G region of Hmg1p was unsuccessful, I focused on determining the molecular characteristics needed for Hmg1p to act as a karmellae signal. We know a subset of the ER-anchored proteins can induce karmellae but not all ER-anchored proteins are capable of eliciting this response from the cell. The proteins, HMGR (Wright *et al.*, 1988), cytochrome P450 (Schunck *et al.*, 1991), cytochrome b5 (Vergeres *et al.*, 1993), canine ribosomal receptor (Wanker *et al.*, 1995), protease B negative 1 (Naik and Jones, 1998), and plant plasma membrane H^+-ATPase (Villalba *et al.*, 1992), can induce karmellae but do not share any sequence homologies. What properties lead to the cell perceiving a signal for increased ER production? In this dissertation, I postulate that these different proteins use a common pathway to signal for ER proliferation. The ER proliferation pathway requires increased levels of an ER-anchored protein which assembles other

lipids and proteins into an ER subcompartment, thereby modifying the composition of the ER. I hypothesize that the cell perceives this altered ER composition as the signal for ER proliferation. The ER composition can be monitored by proteins known to participate in the ER quality control system. The proteins of the ER quality control system are beginning to be identified. Recently, Loayza *et al.* identified Hrd2p, a proteosome subunit, as a component of the ER quality control system in a screen for suppressors which improved the exit from the ER of Ste6p mutants (Loayza *et al.*, 1998). Koning *et al.* demonstrated that the ER subcompartment containing Hmg2p had less Kar2p than other regions of the ER (Koning *et al.*, 1996). I do not know the extent of the variation in composition between ER subcompartments. One way to test for altered ER composition would be to perform immunofluorescence using a panel of antibodies against known ER proteins and determine the co-localization patterns. Another way to identify the components assembled in an ER subcompartment would be to perform cross-linking experiments to determine which proteins were in close physical association with Hmg1p. The cross-linking experiments could be performed on cells that were generating karmellae and on cells expressing a mutant version of Hmg1p unable to induce karmellae to see if the protein profiles were different for the cells with karmellae. The Wright lab also has a 6 His-tagged version of the Hmg1p which is capable of signaling for karmellae. This His-tagged Hmg1p could be used on a talon column to isolate the proteins which associated with Hmg1p under karmellae conditions.

What about a role for lipids?

We describe our model for karmellae signaling as requiring specific protein-protein interactions but the lipid content of the ER may be remodeled as well.

Do karmellae contain an altered lipid profile compared to the rest of the ER? ER membranes could be isolated from yeast generating karmellae and yeast in the uninduced state to determine the lipid composition and abundance of lipid species in these membranes. The Wright lab has started this type of lipid analysis on different yeast strains.

Building on my thesis work

In Chapter 2, I demonstrated that the sequences at the carboxyl terminus of Hmg1p can profoundly affect the ability of this protein to signal for karmellae. Our working hypothesis is that a truncated or misfolded cytosolic domain prevents proper signaling for karmellae by interfering with the required tertiary structure of the membrane domain. Jingami *et al.* had previously shown that deletion of two contiguous membrane-spanning regions from hamster HMGR eliminated the ability of this protein to induce crystalloid ER. These authors postulated that the failure to induce ER proliferation was due to the altered conformation of the membrane domain (Jingami *et al.*, 1987). Future experiments could test the conformation of the membrane domain in the truncated Hmg1p proteins that were unable to generate karmellae. These experiments could check for differences in protease sensitivity between the wild-type Hmg1p and the truncated Hmg1p or use a conformation-specific antibody to test for membrane domain changes. Unfortunately, a conformation-specific antibody would first need to be generated and tested before different proteins could be analyzed. Lastly, a screen for high-copy number suppressors of the truncated Hmg1p proteins could be carried out to find proteins that restore the ability to induce karmellae. The suppressors would be candidates for proteins that interact with Hmg1p or bypass suppressors that induce karmellae without needing Hmg1p. The recovered

suppressors can be tested for their ability to induce karmellae alone in a strain that is not expressing Hmg1p. The current method for isolating high-copy number suppressors that restore karmellae is to visually screen yeast for karmellae by staining with $DiOC_6$.

The sequence or structural requirements for the signaling of karmellae by the ER-anchored proteins are not understood even though a number of different ER membrane proteins have been shown to induce karmellae. These proteins do not contain sequence homologies and do not possess a similar number of membrane-spanning segments. To define the critical amino acids in the karmellae-inducing Hmg1p, I used PCR mutagenesis of the Loop G coding region. In chapter 3, I identified amino acid changes in Loop G of the membrane domain of Hmg1p which reduced the ability of the mutant Hmg1p proteins to signal for karmellae. For three of the most severe mutants, I determined the subcellular localization of the mutant proteins by indirect immunofluorescence. In these cases, the mutant Hmg1p proteins were localized in an ER pattern indistinguishable from the wild-type Hmg1p pattern. Thus, it appears that these amino acid changes did not alter localization of the proteins but reduced karmellae by limiting the signaling ability of the protein. I hypothesize that Loop G serves as a signaling region by mediating protein-protein interactions between Hmg1p and ER-lumenal proteins which leads to a concentration of proteins into an ER subdomain. Because the Loop G mutants generate 9-84% of expected karmellae levels, the altered Loop G sequences are being recognized as karmellae signals at some frequency. The next experiment would be to screen for high copy number suppressors which restore wild-type karmellae levels. These suppressors may compensate for the mutated HMGR and restore karmellae or they may bypass HMGR and signal for karmellae themselves. The protocol for isolation of these suppressors would be identical to the above mentioned $DiOC_6$ screen. Further analysis of the karmellae-

signaling pathway will provide information concerning how a cell monitors the level of a particular membrane protein and responds by coordinating membrane biogenesis.

Bibliography

Alberts, A. W., J. Chen, G. Kuron, V. Hunt, J. Huff, C. Hoffman, J. Rothrock, M. Lopez, H. Joshua, E. Harris, A. Patchett, R. Monaghan, S. Currie, E. Stapley, G. Alberts-Schonberg, O. Hensons, J. Hirschfield, K. Hoogsteen, J. Liesch, and J. Springer. (1980). "Mevinolin: a highly potent competitive inhibitor of hydroxymethylglutaryl-coenzyme A reductase and a cholesterol-lowering agent." Proc. Natl. Acad. Sci. **77**: 3957-3961.

Basson, M. E., R. L. Moore, J. O'Rear, and J. Rine (1987). "Identifying mutations in duplicated functions in Saccharomyces cerevisiae: recessive mutations in HMG-CoA reductase genes." Genetics **117**: 645-655.

Basson, M. E., M. K. Thorsness, J. Finer-Moore, R. Stroud, and J. Rine (1988). "Structural and functional conservation between yeast and human 3-hydroxy-3-methylglutaryl coenzyme A reductases, the rate-limiting enzyme of sterol biosynthesis." Mol. Cell. Biol. **9**: 3797-3808.

Basson, M. L., M. K. Thorsness, and J. Rine. (1986). "Saccharomyces cerevisiae contains two functional genes encoding 3-hydroxy-3-methylglutaryl coenzyme A reductase." Proc. Natl. Acad. Sci. USA **83**: 5563-5567.

Black, V. H. (1972). "The development of smooth-surfaced endoplasmic reticulum in adrenal cortical cells of fetal guinea pigs." Am. J. Anat. **156**: 318-418.

Braunbeck,T. and A. Volkl. 1991. Induction of biotransformation in the liver of the eel (*Anguilla anguilla* L.) by sublethal exposure to dinitro-o-creaol: an ultrastructural and biochemical study. *Toxicol. Environ. Safety.* 21:109-127.

Cadwell, R. C. and G. F. Joyce. (1992). "Randomization of Genes by PCR Mutagenesis." Research **Vol 2**: pp. 28-33.

Casey, W. M., G. A. Keesler, and L.W. Parks. (1992). "Regulation of partitioned sterol biosynthesis in *Saccharomyces cerevisiae*." J. Bacteriol. **174**: 7283-7288.

Chalfie, M., Y. Tu, G. Euskirchen, W. W. Ward, and D. C. Prasher. (1994). "Green fluorescent protein as a marker for gene expression." Science **263**: 802-805.

Chin, D. J., K. L. Luskey, R. G. W. Anderson, J. R. Faust, J. L. Goldstein, and M. S. Brown. (1982). "Appearance of crystalloid endoplasmic reticulum in compactin-resistant Chinese hamster cells with a 500-fold elevation in 3-hydroxy-3-methylglutaryl coenzyme A reductase." Proc. Natl. Acad. Sci. USA. **79**: 1185-1189.

Dallner, G., P. Siekevitz, and G. E. Palade. (1966). "Biogenesis of Endoplasmic Reticulum Membranes." Journal of Cell Biology **30**: 73-96.

Deschenes, R. J. and J. R. Broach (1987). "Fatty acylation is important but not essential for *Saccharomyces cerevisiae RAS* function." Mol. Cell Biol. 7: 2344-2351.

Donald, A., R. Y. Hampton, I. Fritz. (1997). "Effects of Overproduction of the Catalytic Domain of 3-hydroxy-3-methylglutaryl coenzyme A reductase on Squalene Synthesis in *Saccharomyces cerevisiae*." Appl. Envir. Micro. **Vol. 63**(9): pp. 3341-3344.

Edwards, P. A., E. S. Kempner, S. F. Lan, and S. K. Erickson. (1985). "Functional size of rat hepatic 3-hydroxy-3-methylglutaryl coenzyme A reductase as determined by radiation inactivation." J. Biol. Chem. **260**: 10278-10282.

Fowler, A. V. and I. Zabin. (1983). "Purification, Structure, and Properties of Hybrid β-Galactosidase Proteins." J. Biol. Chem. **Vol. 258, No. 23**(Issue of December 10): pp. 14354-14358.

Frimpong, K. and V. W. Rodwell (1994). "The active site of hamster 3-hydroxy-3-methylglutaryl-CoA reductase resides at the subunit interface and incorporates

catalytically essential acidic residues from separate polypeptides." J. Biol. Chem. **269**: 1217-1221.

Gietz, D., A. S. Jean, R. A. Woods, and R. H. Schiestl. (1992). "Improved method for high efficiency transformation of intact yeast cells." Nucleic Acids Research **20**(6): 1425.

Gil, G., J. R. Faust, D. J. Chin, J. L. Goldstein and M. S. Brown. (1985). "Membrane-bound domain of HMG-CoA reductase is required for sterol-enhanced degradation of the enzyme." Cell **41**: 249-258.

Goldstein. J. L. and M. S. Brown (1990). "Regulation of the mevalonate pathway." Nature **343**: 425-430.

Gong, F. C., T. H. Giddings, J. B. Meehl, L. A. Staehelin, and D. W. Galbraith. (1996). "Z-membranes: artificial organelles for overexpressing recombinant integral membrane proteins." Proc Natl Acad Sci U S A **93**(5): 2219-23.

Guarente, L. (1983). "Yeast Promoters and *lacZ* Fusions Designed to Study Expression of Cloned Genes in Yeast." Methods Enzymol. **101**: pp. 181-191.

Hampton, R. Y., R. Gardner, and J. Rine. (1996). "The role of 26S proteasome and HRD genes in the degradation of HMG-CoA reductase, an integral ER membrane protein." Mol. Biol. Cell **7**: 2029-2044.

Hampton, R. Y. and J. Rine (1994). "Regulated degradation of HMG-CoA reductase, an integral membrane protein of the endoplasmic reticulum, in yeast." J. Cell Biol. **125**(2): 299-312.

Howell, N. (1999). "Human mitochondrial diseases: answering questions and questioning answers." Int Rev Cytol **186**: 49-116.

Jingami, H., M. S. Brown, J. L. Goldstein, R. G. W. Anderson, K. L. Luskey. (1987). "Partial deletion of membrane-bound domain of 3-hydroxy-3-methylglutaryl coenzyme A reductase eliminates sterol-enhanced degradation and prevents formation of crystalloid endoplasmic reticulum." J. Cell. Biol. **104**: 1693-1704.

Kochevar, D. and R. G. W. Anderson (1987). "Purified crystalloid endoplasmic reticulum from UT-1 cells contains multiple proteins in addition to 3-hydroxy-3-methylglutaryl coenzyme A reductase." J. Biol. Chem. **262**: 10321-10326.

Koning, A. J., P. Y. Lum, J. Williams, and R. L. Wright (1993). "$DiOC_6$ staining reveals organelle structure and dynamics in living yeast cells." Cell Motil. Cytoskel. **25**: 111-128.

Koning, A. J., C. J. Roberts, and R. L. Wright (1996). "Different subcellular localization of *Saccharomyces cerevisiae* HMG-CoA reductase isozymes at elevated levels corresponds to distinct endoplasmic reticulum membrane proliferations." Mol. Biol. Cell 7: 769-789.

Laemmli, U. K. (1970). "Cleavage of Structural Proteins during the Assembly of the Head of Bacteriophage T4." Nature **227**: 680-685.

Loayza, D., A. Tam, W. K. Schmidt, and S. Michaelis. (1998). "Ste6p Mutants Defective in Exit from the Endoplasmic Reticulum (ER) Reveal Aspects of an ER Quality Control Pathway in *Saccharomyces cerevisiae*." Mol. Biol. Cell **Vol. 9**(October): pp. 2767-2784.

Lum, P. Y., S. Edwards, and R. L. Wright. (1996). "Molecular, functional, and evolutionary characterization of the gene encoding HMG-CoA reductase in the fission yeast, *Schizosaccharomyces pombe*." Yeast **12**: 1107-1124.

Lum, P. Y. and R. Wright (1995). "Degradation of HMG Co-A reductase-induced membranes in the fission yeast, Schizosaccharomyces pombe." J. Cell Biol. **131**(1): 81-94.

Morell, P. (1984). Mvelin. New York, Plenum Press.

Muhlrad, D., R. Hunter, and R. Parker.(1992). "A Rapid Method for Localized Mutagenesis of Yeast Genes." Yeast **8**: 79-82.

Naik, R. R. and E. W. Jones (1998). "The PBN1 Gene of *Saccharomyces cerevisiae*: An Essential Gene That Is Required for the Post-translational Processing of the Protease B Precursor." Genetics **149**: 1277-1292.

Nishikawa, S., A. Hirata, and A. Nakano. (1994). "Inhibition of endoplasmic reticulum (ER)-to-Golgi trasport induces relocalization of binding protein (BiP) within the ER to form Bip bodies." Mol. Bio. Cell **5**: 1129-1143.

Nott, J. A. and M. N. Moore (1987). "Effects of polycyclic aromatic hydrocarbons on molluscan lysosomes and endoplasmic reticulum." Histochem. J. **19**: 357-368.

Parrish, M., C. Sengstag, J. Rine, and R. L. Wright (1995). "Identification of the sequences in HMG-CoA reductase required for karmellae assembly." Mol. Biol. Cell **6**: 1535-1547.

Pathak, R. K., K. L. Luskey, and R. G. W. Anderson. (1986). "Biogenesis of the crystalloid endoplasmic reticulum in UT-1 cells: evidence that newly formed endoplasmic reticulum emerges from the nuclear envelope." J. Cell Biol. **102**: 2158-2168.

Prasher, D. C., V. K. Eckenrode, W. W. Ward, F. G. Prendergast, and M. J. Cormier. (1992). "Primary structure of the *Aequorea victoria* green-fluorescent protein." Gene **111**: 229-233.

Preuss, D., J. Mulholland, C. A. Kaiser, P. Orlean, C. Albright, M. D. Rose, P.W. Robbins, and D. Botstein. (1991). Structure of the yeast endoplasmic reticulum:

localization of ER proteins using immunofluorescence and immunoelectron microscopy. *Yeast.* 7:891-911.

Pringle, J. R., R. A. Preston, A. E. M. Adams, T. Stearns, D. G. Drubin, B. K. Haarer, and E. W. Jones. (1989). "Fluorescence microscopy methods for yeast." Meth. Cell Biol. **31**: 357-435.

Rine, J., W. Hansen, E. Hardeman, and R. W. Davis. (1983). "Targeted selection of recombinant clones through gene dosage effects." Proc. Natl. Acad. Sci. USA **80**: 6750-6754.

Roitelman, J., E. H. Olender, S. Bar-Nun, J. W. A. Dunn, and R. D. Simoni. (1992). "Immunolgical evidence for eight spans in the membrane domain of 3-hydroxy-3-methylglutaryl Coenzyme A reductase: implications for enzyme degradation in the endoplasmic reticulum." J. Cell Biol. **5**: 959-973.

Rose, M. D., F. Winston, and P. Hieter. (1989). Methods in Yeast Genetics. Cold Spring Harbor Laboratories, Cold Spring Harbor, 169.

Rothstein, R. (1991). Targeting, disruption, replacement, and allele rescue: Integrative DNA transformation in yeast. Guide to Yeast Genetics and Molecular Biology. C. Guthrie and G. R. Fink. San Diego, Academic Press.

Schunck, W., F. Vogel, B. Gross, E. Kargel, S. Mauersberger, K. Kopke, C. Gengnagel, and H. Muller. (1991). "Comparision of two cytochromes P-450 from *Candida maltosa*: primary structures, substrate specificities and effects of their expression in *Saccharomyces cerevisiae* on the proliferation of the endoplasmic reticulum." Eur. J. Cell Biol. **55**: 336-345.

Sengstag, C., C. Stirling, R. Schekman, and J. Rine. (1990). "Genetic and biochemical evaluation of eukaryotic membrane protein topology: the polytopic structure of S. cerevisiae HMG-CoA reductase." Mol. Cell. Biol. **10**: 672-680.

Sherman, F., G. R. Fink, and J. B. Hicks. (1986). Methods in Yeast Genetics. Cold Spring Harbor, Cold Spring Harbor Labs.

Shohat, M., G. Janossy, and R. R. Dourmashkin. (1973). "Development of rough endoplasmic reticulum in mouse splenic lymphocytes stimulated by mitogens." Eur. J. Immunol. **3**: 680-687.

Shoubridge, E. A. (1994). "Mitochondrial DNA diseases: histological and cellular studies." J Bioenerg Biomembr **26**: 301-310.

Sikorski, R. S. and P. Hieter (1989). "A uniform set of multipurpose shuttle vectors and yeast host strains designed for efficient manipulation of DNA in *S. cerevisiae*." Genetics **122**: 19-27.

Sisson, J. K. and W. H. Fahrenbach (1967). "Fine structure of steroidogenic cells of a primate cutaneous organ." Am. J. Anat. **121**: 337-368.

Skalnik, D. G., H. Narita, C. Kent, and R. D. Simoni. (1988). "The membrane domain of 3-hydroxy-3-methylglutaryl coenzyme A reductase confers endoplasmic reticulum localization and sterol-regulated degradation onto β-galactosidase." J. Biol. Chem. **263**: 6836-6841.

Spurr, A. R. (1969). "A low-viscosity epoxy resin embedding medium for electron microscopy." Journal of Ultrastructural Research **26**: 31-43.

Thompson, J. D., T. J. Gibson, F. Plewniak, F. Jeanmougin, and D. G. Higgins. (1997). "The CLUSTAL_X windows interface: flexible strategies for multiple sequence alignment aided by quality analysis tools." Nucleic Acids Res **25**(24): 4876-82.

Tsuneoka, M., and E. Mekada. 1992. Degradation of a nuclear-localized protein in mammalian COS cells, using *Escherichia coli* β-galactosidase as a model protein. *J. Biol. Chem.* 267:9107-9111.

Vergeres, G., T. S. B. Yen, J. Aggeler, J. Lausier, and L. Waskell. (1993). "A model system for studying membrane biogenesis: overexpression of cytochrome b_5 in yeast results in marked proliferation of the intracellular membrane." J. Cell Sci. **106**: 249-259.

Villalba, J. M., M. G. Palmgren, G. E. Berberian, C. Ferguson, and R. Serrano. (1992). "Functional Expression of Plant Plasma Membrane H^+-ATPase in Yeast Endoplasmic Reticulum." The Journal of Biological Chemistry **267**(17): 12341-12349.

Von Meyenburg, K., B. B. Jorgensen, and B. V. Deurs. (1984). "Physiological and morphological effects of overproduction of membrane-bound ATP synthase in E. coli K-12." EMBO J. **3**: 1791-1797.

Wanker, E. E., Y. Sun, A. J. Savitz, and D. I . Meyer. (1995). "Functional characterization of the 180-kD ribosome receptor in vivo." J. Cell Biol. **130**: 29-39.

Weiner, J. H., B. D. Lemire, M. L. Elmes, R. D. Bradley, and D. G. Scraba. (1984). "Overproduction of fumarate reductase in Escherichia coli induces a novel intracellular lipid-protein organelle." J. Bacteriol. **158**: 590-596.

Wilkenson, W. O., J. P. Walsh, J. M. Corless, and R. M. Bell. (1986). Crystalline arrays of the Escherichia coli sn-glycerol-3-phosphate acyltransferase, an integral membrane protein. J. Biol. Chem. 261:9951-9958.

Wilson, I. A., H. L. Niman, R. A. Houghten, A. R. Cherenson, M. L. Connolly, and R. A. Lerner. (1984). "The structure of an antigenic determinant in a protein." Cell **37**: 767-778.

Wirtz, K. W. A. and T. W. J. Gadella (1990). "Properties and modes of action of specific and nonspecific phospholipid transfer proteins." Experientia **46**: 592-599.

Wirtz, K. W. A. and D. B. Zilversmit (1968). "Exchange of phospholipids between liver mitochondria and microsomes in vitro." J. Biol. Chem. **243**: 3596-3602.

Wright, R., M. Basson, L. D; Ari, and J. Rine. (1988). "Increased amounts of HMG-CoA reductase induce "karmellae": a proliferation of stacked membrane pairs surrounding the yeast nucleus." J. Cell Biol. **107**: 101-114.

Wright, R., G. Keller, S. J. Gould, S. Subramani, and J. Rine. (1990). "Cell-type control of membrane biogenesis induced by HMG-CoA reductase overproduction." New Biologist **2**: 915-921.

Wright, R. and J. Rine (1989). "Transmission electron microscopy and immunocytochemical studies of yeast: analysis of HMG-CoA reductase overproduction by electron microscopy." Methods in Cell Biol. **31**: 473-512.

Yamamoto, A., R. Masaki, and Y. Tashiro. (1996). "Formation of crystalloid endoplasmic reticulum in COS cells upon overexpression of microsomal aldehyde dehydrogenase by cDNA transfection." J. Cell. Sci. **Vol. 109**: pp. 1727-1738.

Zimmer, T., F. Vogel, A. Ohta, M. Takagi, and W. Schunck. (1997). "Protein Quality-A Determinant of the Intracellular Fate of Membrane-Bound Cytochromes P450 in Yeast." DNA AND CELL BIOLOGY **16**(4): 501-514.

Zucker-Franklin, D., M. F. Greaves, C. E. Grossi, and A. M. Marmont. (1988). Atlas of Blood Cells: Function and Pathology. Milano, edi.Ermes.

VITA

DEBORAH ANN PROFANT

University of Washington

1999

EDUCATION

University of Washington
Interdisciplinary Molecular and Cellular Biology Program and the Department of Zoology
Seattle, WA 98195 — Ph.D. expected
Advisor: Dr. Robin Wright — May 1999

University of California, Santa Cruz — B.A. in Biology
Department of Biology — Highest Honors
Santa Cruz, CA 95064 — June 1992

RESEARCH EXPERIENCE

IMCBP and the Department of Zoology — 6/92-5/99
Seattle, WA 98195
- Graduate Student

Advisor: Dr. Robin Wright

University of California, Santa Cruz — 9/91-3/92
Department of Biology
- Undergraduate Research Internship

Supervisor: Dr. John Tamkun

TEACHING EXPERIENCE

Mentor, University of Washington — Summer 1998
NASA Undergraduate Research Program

Students: Sabrina Andrews and Sarah Prichard

Mentor, University of Washington — Summer 1997
NASA Undergraduate Research Program
Students: Sarah Sager and Annie Alidina

Teaching Assistant, University of Washington — Summer 1997
Biology 401
Instructor: Dr. Robin Wright

Teaching Assistant, University of Washington — Winter 1997
Biology 201
Instructors: Dr. Arnie Bendich and Dr. Luca Comai

Teaching Assistant, University of Washington — Winter 1996
Biology 201
Instructors: Dr. Trisha Davis and Dr. Bonnie Brewer

Teaching Volunteer, University of Washington — Autumn 1996
DNA Sequencing Lab for Garfield High School
Program Coordinator: Molecular Biotechnology

Seminar Participant, University of Washington — Autumn 1996
Graduate Seminar on Teaching, Zoology 529
Moderator: Dr. Jon Herron

Teaching Assistant, University of Washington — Autumn 1995
Biology 402
Instructor: Dr. David Shellenbarger

Teaching Assistant, University of Washington — Autumn 1994
Biology 202
Instructors: Dr. Aimee Bakken and Dr. Robert Steiner

Teaching Assistant, University of Washington — Autumn 1993
Biology 401
Instructors: Dr. Merrill Hille and Dr. Aimee Bakken

HONORS

Department of Defense Fellowship — Winter 1993
Honorable Mention for Graduate Proposal

Priscilla Parkin Memorial Scholarship — 1991-1992
Crown College
University of California, Santa Cruz

PUBLICATIONS

Profant, Deborah, Christopher J. Roberts, Ann J. Koning, and Robin Wright. The role of the HMG-CoA reductase cytosolic domain in karmellae biogenesis. submitted to *Molecular Biology of the Cell* April 1999

Profant, Deborah, Christopher J. Roberts, and Robin Wright. Mutational analysis of the karmellae-inducing signal in HMG-CoA reductase of *Saccharomyces cerevisiae*. submitted to *Yeast* in May 1999

RECENT ABSTRACTS

Profant, Deborah and Robin Wright. 1998. Defining the role of the cytosolic domain of Hmg1p in karmellae biogenesis. Yeast Genetics and Molecular Biology Meeting. Washington, D.C.

Profant, Deborah, Chris J. Roberts, and Robin Wright. 1998. Mutational analysis of the karmellae-inducing signal in the Hmg1p membrane domain. Yeast Genetics and Molecular Biology Meeting. Washington, D.C.

Profant, Deborah. 1997. Mutational analysis of the karmellae-inducing signal. Zoology Graduate Student Symposium. Seattle, WA.

Profant, Deborah and Robin Wright. 1996. Search for proteins that interact with the karmellae-inducing signal of yeast HMG-CoA reductase. The American Society for Cell Biology Meeting. San Francisco, CA.

IMAGE EVALUATION TEST TARGET (QA-3)

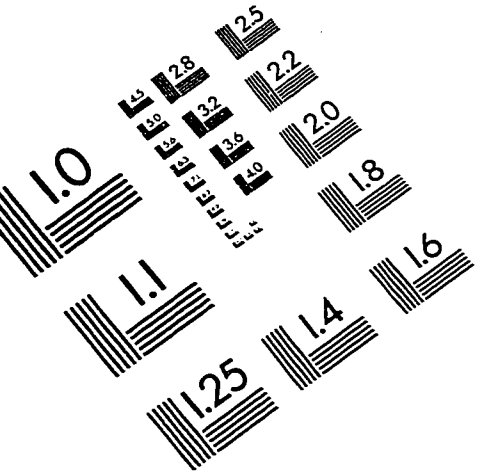

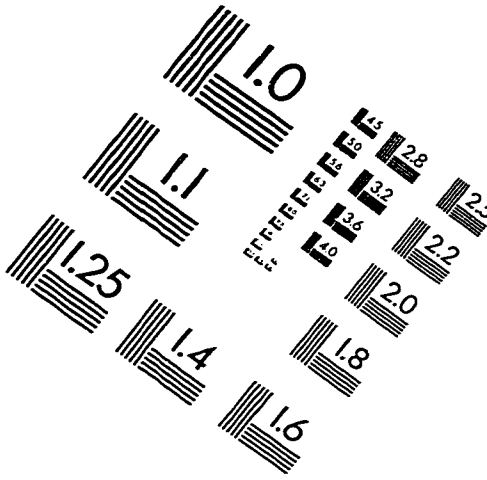

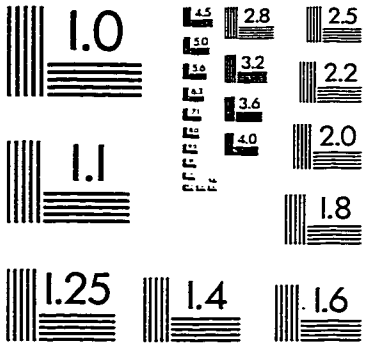

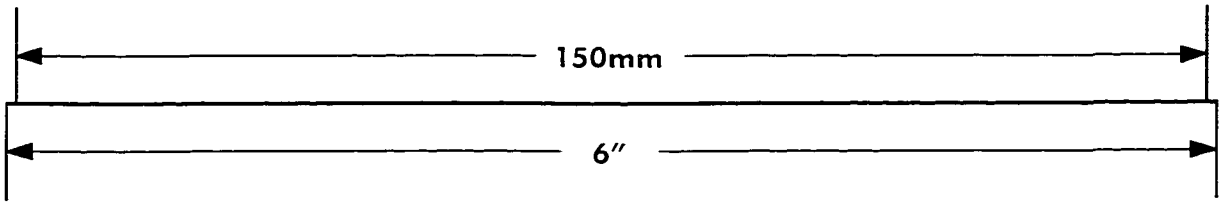

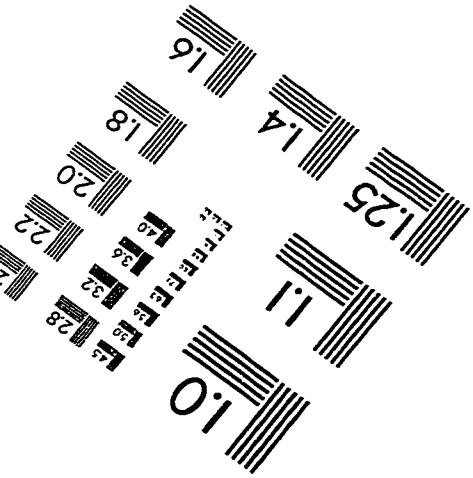

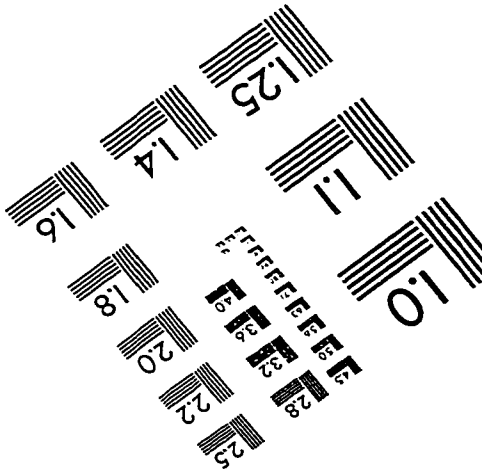

APPLIED IMAGE, Inc
1653 East Main Street
Rochester, NY 14609 USA
Phone: 716/482-0300
Fax: 716/288-5989